67th Meeting of the AEROBALLISTIC RANGE ASSOCIATION
Toledo, Spain, October 2 -7, 2016

Design of a Two-Stage Light Gas Gun for Muzzle Velocities of 10 - 11 km/s

David W. Bogdanoff

Analytical Mechanics Associates, Inc.
NASA Ames Research Center
Moffett Field, CA 94035-0001

ABSTRACT

Space debris poses a major risk to spacecraft. In low earth orbit, impact velocities can be 10 – 11 km/s and as high as 15 km/s. For debris shield design, it would be desirable to be able to launch projectiles of known shape and mass to these velocities. The design of the proposed 10 – 11 km/sec gun uses, as a starting point, the Ames 1.28”/0.22” two stage gun, which has achieved muzzle velocities of 10 – 11.3 km/sec. That gun is scaled up to a 0.3125” launch tube diameter. The gun is then optimized with respect to maximum pressures by varying the pump tube length to diameter ratio (L/D), the piston mass and the hydrogen pressure. A pump tube L/D of 36.4 is selected giving the best overall performance. Piezometric ratios for the optimized guns are found to be ~2.3, much more favorable than for more traditional two stage light gas guns, which range from 4 to 6. (The piezometric ratio for a gun is defined as the maximum projectile base pressure divided by the constant projectile base pressure which, acting over the entire barrel length, would produce the same muzzle velocity.) The maximum powder chamber pressures are 20 to 30 ksi. To reduce maximum pressures, the desirable range of the included angle of the cone of the high pressure coupling is found to be 7.3 to 14.6 degrees. Lowering the break valve rupture pressure is found to lower the maximum projectile base pressure, but to raise the maximum gun pressure. For the optimized gun with a pump tube L/D of 36.4, increasing the muzzle velocity by decreasing the projectile mass and increasing the powder loads is studied. It appears that saboted spheres could be launched to 10.25 and possibly as high as 10.8 km/sec, and that disc-like plastic models could be launched to 11.05 km/s. The use of a tantalum liner to greatly reduce bore erosion and increase muzzle velocity is discussed. With a tantalum liner, CFD code calculations predict muzzle velocities as high as 12 to 13 km/s.

I. INTRODUCTION

Space debris poses a major risk to spacecraft. In low earth orbit, crossed orbits produce impact velocities of 10 – 11 km/s and directly opposed orbits produce impact velocities up to 15 km/s. To design effective debris shields, it would be desirable to launch projectiles of known shapes in the ballistic range to these velocities. (Projectiles of glass, aluminum or other materials would be of interest.) A first step towards that goal would be to attain the 10 – 11 km/s velocity range. A stable of four two stage light gas guns with launch tube diameters ranging from 0.28” to 1.5” is available at the NASA Ames Research Center (A sketch of representative configuration

of a two stage light gas gun is shown in Fig. 1.) The Ames guns are of a very similar design with pump tube length to diameter ratios (L/Ds) of 208 to 273. These guns have achieved maximum muzzle velocities with slug projectiles ranging from 8.44 to 9.46 km/s. However, with a saboted sphere projectile, the maximum muzzle velocity achieved (for the 0.5" gun) was 8.2 km/s. Thus, the four standard guns in the Ames stable cannot reach the desired muzzle velocities. The maximum velocities of these 4 Ames guns are reasonably representative of those of most two stage light gas guns at various laboratories around the world.

The design of the proposed 10 – 11 km/sec gun would use, instead, as a starting point, the design of the Ames 1.28"/0.22" two stage gun, which has achieved muzzle velocities of 9.8 – 11.3 km/sec, depending on the launch package mass, but is no longer available. It is proposed that the Ames 1.28"/0.22" gun be scaled up by a factor of 1.420 to have a launch tube diameter of 0.313". The scale up would permit the use of 0.313" high pressure tubing as an expendable launch tube – high pressure tubing is not available with a 0.22" diameter. Herein, for brevity, we will refer to the proposed 10 – 11 km/sec gun as a "10 km/s gun" and denote its various embodiments by the notation "P10". We will denote the Ames 1.28"/0.22" two stage gun by the designation "Ames HV." When other Ames guns are discussed, the launch tube or launch tube and pump tube diameters will be given.

All CFD calculations herein are performed using a higher-order Godunov CFD code described in Refs. 1 and 2, as implemented in Ref. 2. This version of the code models the erosion of the gun tube material and the incorporation of the eroded wall material into the hydrogen working gas. It was shown in Ref. 2 that the gun tube erosion and metal loading of the hydrogen working gas must be taken into account to model shots at muzzle velocities above roughly 7 km/s. In Refs. 1 and 2, CFD code validation against experimental data for muzzle velocities of 5.4 to 9.4 km/s is presented. The guns with which the validations were performed had launch tube diameters ranging from 0.28" to 1.50". Later code validations (unpublished) have extended the code validation to muzzle velocities ranging from 3 to 11.3 km/s.

Section A below sets up the first version of the P10 gun selects and the optimum gunpowder to be used. Section B through I deal with optimizations of the gun with respect to pump tube length to diameter ratio (L/D), piston mass and hydrogen pressure. Section J discusses optimization of the angle of the high pressure coupling contraction cone. Section K discusses the effect of varying the projectile mass. Section L discusses the effect of varying the break valve rupture pressure. Section M discusses a possible pump tube diameter effect. Section N presents key parameters of optimized guns for various pump tube L/Ds. Sections O and P discuss ways to increase the gun muzzle velocity above 10 km/s. Section O discusses decreasing the projectile mass and increasing the powder load. Section P discusses the use of a refractory metal liner. Finally, Section III presents a summary and the conclusions.

II. OPTIMIZATION OF P10 GUN

A. First assessment of P10 gun performance at the baseline scaled-up operating condition

The dimensions and operating parameters for the Ames HV gun are directly scaled up for the first version of the P10 launcher. The performance and operating parameters of the Ames HV gun are given in Refs. 3 and 4. Corresponding data for a very similar gun is given in Ref. 5. The break valve rupture pressure is not given in Refs. 3 and 4, but a value of 20 ksi is given in Ref. 5. For the bulk of the calculations herein, we have used, instead of 20 ksi, a value of 27.5 ksi, which produces CFD calculated muzzle velocities in better agreement with the experimental values. The performances of the P10 gun at the baseline scaled-up operating conditions with several different IMR powders are compared with the corresponding performance of the Ames HV gun. (IMR stands for Improved Military Rifle and refers to a series of powders developed by DuPont,

starting in the 1920's.) The parameters for the Ames HV gun and the first embodiment of the P10 gun are given in Table 1.

Table 1. Parameters for Ames HV gun and first version of P10 gun.

Gun	Ames HV	P10
Powder	IMR 4227	IMR various
Powder mass, g	70 - 89	235 - 269.4
Piston mass, g	100	286.6
Hydrogen pressure, psia	40	40
Pump tube L/D	115	115
Diaphragm break pressure, ksi	27.5	27.5
HPC cone angle, degrees	14.6	14.6
Projectile mass, g	0.0756	0.2167
Powder chamber volume, cm^3	1957.3	5609.7

The powder masses, piston mass, projectile mass and powder chamber volume for the P10 gun are simply those for the Ames HV gun scaled up by a factor of the launch tube diameter cubed or $(0.3125/0.22)^3 = 2.866$. The remaining parameters, except for the powders used, are the same for the two guns. For both guns, the piston is taken to be polyethylene and the projectile a Lexan slug. Figure 2 shows two pistons (not to scale). The upper piston is the actual piston, with a conical Bridgeman seal on the front of the piston. The lower piston is a one-dimensional piston version (obligatory for the one-dimensional CFD code) with the correct piston mass and the correct bearing areas on the front and rear piston lands. The static coefficient of friction for the piston is taken to be 0.094. The preceding piston discussion also applies to both guns.

Figure 3 shows the muzzle velocities obtained as a function of the normalized (to the Ames HV gun) powder mass for the two guns. A single curve for the Ames HV gun along with seven different curves for the P10 gun for eight different IMR powders are shown. Figure 4 shows the maximum muzzle velocities obtained in Fig. 3 plotted versus the web size of the powder grains. For the cylindrical powder grains of these powders with one concentric cylindrical perforation, the web size is the outside diameter minus the perforation diameter divided by two. Basically, the web size is the minimum original wall thickness of the powder grain. The linear (inches per second) powder burn rate equation is the same for all of the IMR powders, but the rate of consumption of the powder grains depends on the grain size, being faster for the smaller grain powders. The initial web size is the main factor determining the consumption rate of the grains, the initial grain length having only a minor effect. The powders with the smaller initial web sizes will burn faster. For the IMR powders, the burn rate equation, the grain dimensions and other key powder parameters are given in Ref. 6. In the CFD code, one starts with the initial powder grain shape and, then, all surfaces of the grain are taken to retreat at a rate obtained using the linear burn rate equation.

The highest muzzle velocities are obtained with the best match of the hydrogen compression rate by the piston with the acceleration of the projectile. The object is, as much as possible, to maintain the driving pressure on the projectile. The acceleration history of the piston by the burning powder has a significant effect on the resulting compression of the hydrogen. The flow is, however, very complex and there is no simple way to select, a priori, the powder with the

correct web size to yield the highest muzzle velocity. Rather, complete CFD gun cycle calculations must be performed for each powder. Such calculations were performed, yielding the data shown in Figs. 3 and 4. With a broad range of web sizes, one would expect the behavior described in the following sentences. The smallest web size (fastest) powders will be too fast for the gun system in question, and will give relatively poor performance. Likewise, the largest web size (slowest) powders will be too slow for the gun system in question, and will also give relatively poor performance. The best performance (highest muzzle velocity) would be expected to be obtained with an intermediate web size and powder burn rate.

With the preceding paragraphs as background, we now further discuss Figs. 3 and 4. The first point to note is that simply going from the Ames HV gun to the P10 gun, with the 4227 powder produce a large drop in muzzle velocity, from ~10.15 km/s to ~9.6 km/s. Basically, the 4227 powder burns far too fast for the larger gun. The performance of seven other IMR powders are shown in Figs. 3 and 4. The 4227 and 4198 powders are too fast and the 4831 powder is too slow. Powders with intermediate web sizes and burn rates, the 3031, 4895, 4064, 4320 and 4350 powders, produce improved performance over the 4227 powder. We choose the 4320 powder for further study because it produces the highest muzzle velocity (~9.9 km/s) and also, does not have the abrupt fall-off seen with the 3031 powder. With the 4320 powder, we have gained about 0.3 km/s over the 4227 powder, but are still about 0.25 km/s below the performance of the Ames HV gun with 4227 powder. Further increases in muzzle velocity can be obtained by optimizing the hydrogen pressure, piston mass and pump tube length. These will be studied in succeeding sections.

B. Optimization of P10 gun with respect to hydrogen pressure and piston mass for a pump tube L/D of 115

All of the calculations in this section are for the P10 gun with the IMR 4320 powder, chosen as described in Sec. IIA. The calculations done for the 4320 powder in Sec. IIA were done for a hydrogen pressure of 40 psia and the baseline piston mass. In this section, we discuss calculations done for the following gun operating conditions:

Table 2. Gun operating conditions studied for P10 gun with pump tube L/D = 115.

Hydrogen pressure (psia)	Relative piston mass (1.0 = baseline)	10 km/s reached?	Number of runs
22.5	1.0	No	6
30	1.0	Yes	6
34.6	1.0	Yes	6
40	1.0	No	6
53.3	1.0	No	6
30	0.75	Yes	8
32.2	0.75	Yes	10
34.6	0.75	Yes	10
30	0.56	Yes	8
34.6	1.33	No	6
			TOTAL = 72

The main variables are hydrogen pressure and piston mass. For each of the 10 combinations of hydrogen pressure and piston mass, the powder mass is varied to yield curves of maximum gun pressure and maximum model base pressure versus muzzle velocity. (Due to space limitations, we do not show these plots herein.) The number of runs made for each curve are shown in the

last column of the table. If the two curves cross over 10 km/s, the two pressures at 10 km/s are each interpolated between the two points bracketing 10 km/s and the interpolated pressures are noted down for future discussion. (For example, for the case with the baseline piston mass and 34.6 psia hydrogen pressure, the pressure curves crossed over 10 km/s between the fourth and fifth data points. The two pressures were then interpolated between these two data points.) If the curves fail to reach 10 km/s, that combination of hydrogen pressure and piston mass is rejected for any further consideration.

Figure 5 shows a cross plot of the two maximum pressures at the points where the maximum pressure-muzzle velocity curves reach a 10 km/s muzzle velocity. Six data points for the P10 gun, corresponding to the six sets of gun operating conditions in Table 2 where 10 km/s is reached, are plotted in Fig. 5, along with one point for the Ames HV gun. The larger numbers by data points or lines in Fig. 5 are the hydrogen pressure in psia; the smaller numbers are the normalized piston mass. The condition judged to be the best for the P10 gun in Fig. 5 is the condition with a hydrogen pressure of 32.2 psia and a piston mass of 0.75 times the baseline value. (This data point is circled with a red circle in the graph.) The basic methodology herein for defining the best operating condition is to move toward a condition with the lowest possible maximum projectile base pressure without a substantial increase in the maximum gun pressure. Further discussion of this selection methodology is presented in Sec. F. For this condition, at 10 km/s, the P10 gun has the maximum projectile base pressure 18.5% higher than the Ames HV gun and the maximum gun pressure 9.2% higher than the Ames HV gun. We note that the change of the piston mass from baseline to 0.75 times baseline has very different effects upon the maximum pressures for hydrogen pressures of 30 and 34.6 psia. This is related to the fact that the pressure history at the break valve consists, in general, in a series of very spiky shock waves followed by rarefactions. (For an example, see Ref. 7.) If the gun operating conditions change so that the pressure peak at which the break valve ruptures changes, there can be major changes in the characteristics of the CFD solution.

C. Optimizations of P10 gun with respect to hydrogen pressure and piston mass for a pump tube L/Ds of 153.3 and 86.3.

The optimization of the P10 gun for a pump tube L/D of 115 discussed in Sec. IIB was repeated for pump tube L/Ds of 153.3 and 86.3. These pump tube L/Ds are equal to 1.33 and 0.75 times the baseline value, respectively. Tables 3 and 4 below give the gun operating conditions studied for these two pump tube L/Ds.

Table 3. Gun operating conditions studied for P10 gun with pump tube L/D = 153.3.

Hydrogen pressure (psia)	Relative piston mass (1.0 = baseline)	10 km/s reached?	Number of runs
22.5	1.0	Yes	5
26	1.0	Yes	5
30	1.0	No	6
34.6	1.0	No	7
22.5	0.75	Yes	4
24.2	0.75	Yes	7
26	0.75	Yes	7
22.5	1.33	Yes	7
26	1.33	No	9
			TOTAL = 57

Table 4. Gun operating conditions studied for P10 gun with pump tube L/D = 86.3.

Hydrogen pressure (psia)	Relative piston mass (1.0 = baseline)	10 km/s reached?	Number of runs
34.6	1.0	Yes	7
40	1.0	Yes	8
34.6	0.75	Yes	9
40	0.75	Yes	8
46.2	0.75	Yes	7
53.3	0.75	Yes	6
			TOTAL = 45

Figure 6 corresponds to Fig. 5 given previously, but shows results for all three pump tube L/Ds, 86.3, 115 and 153.3. The best data points for the three pump tube L/Ds are circled with red circles. The best data point for L/D = 153.3 is only very slightly different (slightly worse) than the best data point for L/D = 115. The maximum projectile base pressures for all three L/Ds range from 15 to 18.5% greater than that for the Ames HV gun. The maximum gun pressures for L/D = 153.3 and 115 are 9.2 to 12% greater than that for the Ames HV gun. By shortening the pump tube L/D from 115 to 86.3, there is a reduction of the maximum gun pressure by 10.6% bringing it a level 2.4% below the value for the Ames HV gun.

D. Optimizations of the P10 gun with respect to hydrogen pressure and piston mass for a pump tube L/Ds of 64.7 and 48.5.

The optimization of the P10 gun was repeated for pump tube L/Ds of 64.7 and 48.5. These pump tube L/Ds are equal to 0.563 and 0.422 times the baseline value, respectively. Tables 5 and 6 below give the gun operating conditions studied for these two pump tube L/Ds. Figure 7 corresponds to Fig. 6, and shows results for pump tube L/Ds of 86.3, 64.7 and 48.5. Thus, there is an overlap between Figs. 6 and 7 in that both figures show results for L/Ds of 86.3. The best data points for the three pump tube L/Ds of Fig. 7 are again circled with red circles. Briefly

Table 5. Gun operating conditions studied for pump tube L/D = 64.7.

Hydrogen pressure (psia)	Relative piston mass (1.0 = baseline)	10 km/s reached?	Number of runs
40	1.0	Yes	6
46.2	1.0	Yes	6
53.3	1.0	Yes	8
61.6	1.0	Yes	6
71.1	1.0	Yes	5
82.1	1.0	Yes	6
94.8	1.0	Yes	4
109.5	1.0	Yes	4
126.4	1.0	Yes	4
94.8	0.75	Yes	5
109.5	0.75	Yes	5
94.8	1.33	Yes	5
109.5	1.33	Yes	5
			TOTAL = 69

reviewing the results of Fig. 6, we consider the three maximum projectile base pressures and the three maximum gun pressures for the red circled data points for the P10 gun. Of these pressures, five are higher than those for the Ames HV gun, while only one – the maximum gun pressure for L/D = 86.3 is lower (by 2.4%) than that for the Ames HV gun. By contrast, from Fig. 7, for the red circled data points for L/D = 64.7 and 48.5, all four maximum pressures are lower for the P10 gun than for the Ames HV gun. For the maximum gun pressure, the pressure reduction is modest (2.8%) for L/D = 64.7, but significant (15.2%) for L/D = 48.5. For the maximum projectile base pressures, the pressure reductions below those of the Ames HV gun are substantial (25.1% and 40.3%, respectively, for L/D = 64.7 and 48.5).

Table 6. Gun operating conditions studied for pump tube L/D = 48.5.

Hydrogen pressure (psia)	Relative piston mass (1.0 = baseline)	10 km/s reached?	Number of runs
71.1	1.0	Yes	5
82.1	1.0	Yes	6
94.8	1.0	Yes	6
109.5	1.0	Yes	6
126.4	1.0	Yes	5
146.0	1.0	Yes	4
168.6	1.0	Yes	4
194.6	1.0	Yes	5
224.8	1.0	Yes	4
259.6	1.0	Yes	6
194.6	0.75	Yes	4
224.8	0.75	Yes	6
194.6	1.33	Yes	6
224.8	1.33	Yes	5
			TOTAL = 72

E. Optimizations of P10 gun with respect to hydrogen pressure and piston mass for a pump tube L/Ds of 36.4 and 27.3.

The optimization of the P10 gun was repeated for pump tube L/Ds of 36.4 and 27.3. These pump tube L/Ds are equal to 0.316 and 0.237 times the baseline value, respectively. Tables 7 and 8 below give the gun operating conditions studied for these two pump tube L/Ds. Figure 8 corresponds to Fig. 7, and shows results for pump tube L/Ds of 48.5, 36.4 and 27.3. There is an overlap between Figs. 7 and 8 in that both figures show results for L/Ds of 48.5. The data points judged to be the best for the three pump tube L/Ds of Fig. 8 are again circled with red circles. The decreases in maximum pressures noted previously for the decreasing L/Ds of 86.3, 64.7 and 48.5 continue, to some extent, for the still smaller L/Ds of 36.4 and 27.3. For L/Ds of 86.3, 64.7, 48.5, 36.4 and 27.3, the corresponding maximum gun pressures are 2.4, 2.8, 15.2, 22.4 and 22.4%, respectively, less than that for the Ames HV gun. The corresponding numbers for the maximum projectile base pressures are -15.0, 25.1, 40.3, 45.4 and 48.0%, respectively. (The negative value means that the maximum projectile base pressure is greater for the P10 gun than for the Ames HV gun.)

Table 7. Gun operating conditions studied for pump tube L/D = 36.4.

Hydrogen pressure (psia)	Relative piston mass (1.0 = baseline)	Curve crosses 10 km/s line?	Number of runs
146.0	1.0	Yes	4
168.6	1.0	Yes	4
194.6	1.0	Yes	4
224.8	1.0	Yes	4
259.6	1.0	Yes	5
299.7	1.0	Yes	5
346.0	1.0	Yes	5
399.6	1.0	Yes	5
299.7	0.75	Yes	4
346.0	0.75	Yes	3
299.7	1.33	Yes	4
346.0	1.33	Yes	5
			TOTAL = 52

Table 8. Gun operating conditions studied for pump tube L/D = 27.3.

Hydrogen pressure (psia)	Relative piston mass (1.0 = baseline)	Curve crosses 10 km/s line?	Number of runs
194.6	1.0	Yes	5
224.8	1.0	Yes	4
259.6	1.0	Yes	4
299.7	1.0	Yes	5
346.0	1.0	Yes	4
399.6	1.0	Yes	5
461.4	1.0	Yes	5
532.7	1.0	Yes	4
615.2	1.0	Yes	5
710.3	1.0	Yes	4
461.4	0.75	Yes	5
532.7	0.75	Yes	4
615.2	0.75	Yes	4
532.7	1.33	Yes	5
615.2	1.33	Yes	6
615.2	0.56	Yes	4
			TOTAL = 73

F. Further discussion of criteria for selecting "best" or optimum gun operating conditions.

For Figs. 5 and 6, with pump tube L/Ds of 153.3, 115 and 86.3, the basic methodology herein for defining the best operating condition is to move toward a condition with the lowest possible maximum projectile base pressure without a substantial increase in the maximum gun pressure. As can be seen from the figures, this does not mean that both pressures for each case are simultaneously the absolute minimum values.

For pump tube L/Ds of 64.7 and 48.5 (see Fig. 7), the following methodology was used. With the baseline piston mass, the hydrogen pressure was increased until the maximum projectile base

pressure ceased decreasing and one or both of the two maximum pressures started to rise. Then, at that point, the effect of switching to heavier (1.33 times the baseline piston mass) and lighter (0.75 times the baseline piston mass) piston was studied. Using the heavier piston resulted in a significant increase in the maximum gun pressure with little or no reduction in the maximum projectile base pressure and was rejected as a useful option. Using the lighter piston resulted in a decrease in the maximum gun pressure at the cost of an increase in maximum projectile base pressure. In spite of this, the baseline piston mass is used to define the best operating condition for the present study. The possibility of reducing the maximum gun pressure at the cost of increasing the maximum projectile base pressure by using a lighter piston is noted.

Figure 8 shows results for pump tube L/Ds of 36.4 and 27.3 (as well as repeating the results for L/D = 48.5 shown also in Fig. 7). The criteria for selecting the best operating condition discussed above for L/D = 64.7 and 48.5 also applies for the case with L/D = 36.4. For L/D = 27.3, the situation is not quite as clear, since the maximum gun pressure rises continually while the maximum projectile base pressure falls as the hydrogen pressure increases. We reject the point at a hydrogen pressure of 615.2 psia with the baseline piston mass since it has a significantly higher maximum gun pressure than the point at 532.7 psia pressure and is very close in pressure to the point at 710.3 psia pressure where the maximum projectile base pressure rises sharply. We also reject the point at 0.75 times the baseline piston mass and 615.2 psia pressure because it is very close in piston mass to the point at 0.56 times the baseline piston mass and 615.2 psia pressure, which has a much higher maximum projectile base pressure. Hence, the point at 532.7 psia pressure with the baseline piston mass was judged to be the best operating condition for L/D = 27.3.

There are some judgment calls in selecting the best gun operating conditions, particularly for L/D = 36.4 and 27.3, but it is the author's opinion that the choices made herein result in a fairly accurate assessment of the effect of pump tube length on gun performance.

G. Comparison of optimum operating conditions for P10 gun at various pump tube lengths.

Figure 9 shows the comparison of the optimum gun operating conditions for all seven pump tube lengths. The data points shown are the red circled data points from Figs. 5 through 8. The data point for the Ames HV gun seen in Figs. 5 to 8 is also shown. In addition, the highest velocity experimental data point for the Ames 0.5"/2.535" gun is shown in Fig. 9. For this data point, the pressures are the CFD calculated values for the muzzle velocity of 9.41 km/sec. (The experimental muzzle velocity was less than 1% different – 9.46 km/sec.) Figure 9 also shows an alternative data curve for conditions which can be achieved for L/D = 27.3 to 64.7 with a lighter piston of 75% of the mass of the baseline piston. As was discussed in Sec. IIF, it is seen that lower maximum gun pressures can be achieved with the lighter piston at the cost of increasing the maximum projectile base pressure. Other than the discussion of Sec. IIF and the present discussion of Fig. 9, we will not further discuss the alternative data curve herein. The following sections will deal only with data corresponding to the P10 "Best operating condition curve" in Fig. 9 and the two Ames gun data points shown in the figure.

From Fig. 9, we start off by noting that the Ames HV gun (which is no longer available) is very much superior to the Ames 0.5" gun. The Ames HV gun has a muzzle velocity of 10.0 km/sec versus 9.41 km/sec (both CFD values) for the Ames 0.5" gun and maximum pressures 21 to 26% less than that of the Ames 0.5" gun. The Ames 0.5" gun is typical of the current stable of guns (1.5", 1.0", 0.5" and 0.28") in the Ames HFFAF (Hypervelociy Free Flight Aerodynamic Facility), which have pump tube L/Ds of 208 to 273. The Ames 0.5" gun has achieved the highest muzzle velocity of the 4 currently available HFFAF guns.

From Fig. 9, with the exception of a slightly lower maximum gun pressure for L/D = 86.3, the P10 guns with L/D = 153.3, 115 and 86.3 are inferior to the Ames HV gun. On the other

hand, the P10 guns with L/D = 64.7, 48.5, 36.4 and 27.3 are superior to the Ames HV gun. Since the reductions in maximum pressures are small going from L/D = 36.4 to L/D = 27.3, and the hydrogen pressures (and the corresponding powder pressures) are considerably higher for L/D = 27.3 than for L/D = 36.4, it is the author's opinion that L/D = 36.4 is a good candidate to be the optimum pump tube length for the P10 gun. For L/D = 36.4, the hydrogen pressure is 346 psia and the maximum powder pressure is 20.6 ksi. For L/D = 27.3, by contrast, the hydrogen pressure is 533 psia and the maximum powder pressure is 29.3 ksi.

H. Piezometric ratios and projectile base pressure histories.

The piezometric ratio for a gun is defined as the maximum projectile base pressure divided by the constant projectile base pressure which, acting over the entire barrel length, would produce the same muzzle velocity. The ballistician's ideal constant base pressure gun would have a piezometric ratio of 1.0. Military powder guns typically have piezometric ratios of about 2 (Ref. 8). Typical high performance two stage light gas guns have piezometric ratios of 4 to 6. Using elementary mechanics, it can easily be shown that the equivalent constant base pressure for a gun operating condition is given by

$$p_{cbp} = \frac{2}{\pi}\frac{mv^2}{LD^2} \qquad (1)$$

where:

p_{cbp} = equivalent constant base pressure
m = projectile mass
v = muzzle velocity
L = barrel length
D = barrel inside diameter

Figure 10 shows the piezometric ratios for the P10 and Ames guns plotted versus the pump tube L/D values. "Projectile base" values (left side ordinate scale) are the conventional piezometric ratios. "Gun" values (right side ordinate scale) are a non-conventional piezometric ratio based on the maximum pressure at any location in the gun. For all guns except the Ames 0.5" gun, the ratio of the pump tube diameter to the launch tube diameter is 5.82. However, for the Ames 0.5" gun, this value is 5.07. For this reason, the data points for the latter gun are plotted with two different values of the pump tube L/D. The rightmost ("True L/D") data points for the Ames 0.5" gun are plotted with the actual physical pump tube L/D. However, it may be argued that when the pump tube/launch tube diameter ratios are different, as they are for this case, the correct comparison should be using the pump tube volume normalized by the launch tube diameter cubed rather than the pump tube L/D. Hence, the second set of points [the leftmost ("Vol equiv L/D") points] for the Ames 0.5" gun are plotted at the L/D for a pump tube with a diameter 5.82 times the launch tube diameter with a volume equal to that of the actual pump tube, which has a smaller diameter.

The relations between the maximum gun and projectile base pressures for the P10 guns and the Ames guns shown in Fig. 10 are the same as those shown in Fig. 9. Figure 10, however, shows the maximum pressures as piezometric ratios and plotted directly versus pump tube L/D. In particular, for the two Ames guns and for the three P10 guns with L/D = 153.3, 115 and 86.3, the projectile base piezometric ratios are in the range of 4 to 6, which is typical for high performance two stage light gas guns. However, for the P10 guns with L/D = 64.7, 48.5, 36.4 and 27.3, the projectile base piezometric ratios are much more favorable, being 3.27, 2.54, 2.32

and 2.20, respectively. The lowest two values approach the values for military powder guns. The piezometric ratios based on the maximum gun pressures are also seen to decrease as the pump tube L/D decreases.

Figure 11 shows pressure histories at the projectile base for the P10 guns. These are for the conditions corresponding to the data points of Fig. 10 for the P10 guns. (Note that time origins for the various curves of Fig. 11 are not the true values for the CFD calculations, but rather, have been shifted by arbitrary amounts to allow the seven curves to be shown in one plot.) In general, as the pump tube L/D decreases, the maximum projectile base pressures and the piezometric ratios decrease (see Figs. 9 and 10), the pressure peaks become less spiky and the high pressures are maintained for longer times (which corresponds to being maintained further along the launch tube), leading to improved (reduced) piezometric ratios.

I. Maximum gun pressures plotted versus distance along gun and maximum powder chamber pressures.

For the P10 gun with a pump tube L/D of 36.4, Figure 12 shows the maximum pressures reached at any time in the gun firing cycle plotted versus distance along the gun. Such plots are needed to select the tube wall thicknesses for various parts of the gun. The tubing pressure limits shown are roughly equivalent to the limits given by various manufacturers of high pressure tubing and are not to be taken as exact data.

Figure 13 shows the maximum powder chamber pressures for all seven P10 gun configurations, the Ames 0.5” gun and the Ames HV gun, plotted versus pump tube L/D. This graph shows clearly that the more favorable projectile base and gun maximum pressures and piezometric ratios seen in Figs. 9 to 11 for the P10 guns with the smaller pump tube L/Ds require higher powder chamber pressures. The maximum pressures along the pump tube tend to follow the same trends, averaging roughly half of the powder chamber pressures up to the point where much higher pressures occur due to shock reflection. We note that the highest maximum powder chamber pressures seen in Fig. 13 are 20 to 30 ksi, which is well below representative maximum powder chamber pressures of high performance military gun systems, which can be from 45 to 60 ksi (Ref. 8).

J. Maximum gun pressures and projectile base pressures plotted versus the high pressure coupling contraction cone included angle.

Figure 14 shows the maximum gun pressures and maximum projectile base pressures for the P10 gun with pump tube L/D = 48.5 plotted versus the high pressure coupling contraction cone included angle. We note that the maximum pressures increase sharply as the cone angle decreases below 7.3 degrees. As the cone angle increases above 10.3 degrees the maximum projectile base pressure increases while the maximum gun pressure decreases slightly. We define a “sweet spot” between cone angles of 7.3 and 14.6 degrees. To keep the amount of work within reasonable bounds, the cone angle optimization was not performed for all pump tube L/Ds. The shape of the curves for the maximum pressures may be somewhat different for different pump tube L/Ds. Most of our surveys were done with a cone angle of 14.6 degrees. From Fig. 14, we can see that, for an L/D of 48.5, a reduction of the maximum gun pressure of about 6.5% could be made by changing the cone angle from 14.6 degrees to 10.3 degrees. We do not know exactly the reductions which would be obtained for other L/Ds. Again, to keep the work within bounds, it was decided not to repeat the 500 or so CFD calculations made changing to the 10.3 degrees cone angle. About 60% of the 48 guns described in Ref. 3 have cone angles within our “sweet spot” of 7.3 – 14.6 degrees. However, some of the remaining 40% of the guns have cone angles well outside this range.

K. Projectile mass effect.

Five basic cases were studied, one for the Ames HV gun and four for four configurations of the P10 gun. For each of the five cases studied, all gun operating parameters were held constant except that CFD solutions for three different projectile masses were obtained. For the Ames HV gun, the first basic case for the projectile mass study was a condition very similar to that shown in Figs. 5 - 8, but at a slightly higher powder mass, so that the muzzle velocity was 10.15 km/sec instead of 10.00 km/sec. The projectile masses studied were 0.0453, 0.0756 and 0.0838 g. For the P10 gun configurations, the four basic cases were the optimum operating conditions shown in Figs. 5 – 8 for pump tube L/Ds of 115, 64.7, 48.5 and 36.4. For each case, projectile masses of 0.1299, 0.2167 and 0.2374 g were studied. These masses are equal to the masses for the Ames HV gun multiplied by the ratio of the launch tube diameters cubed. For all five basic cases, the break valve rupture pressure was 27.5 ksi.

The curves of muzzle velocity versus projectile mass for the four P10 gun configurations plus the curve for the Ames HV gun are shown in Fig. 15. The muzzle velocity varies as the projectile mass to a power between -0.100 and -0.165. The curves of maximum projectile base pressure versus projectile mass for the five gun configurations are shown in Fig. 16. The maximum projectile base pressure varies as the projectile mass to a power between 0.58 and 1.07. We note that the maximum gun pressures vary only very slightly (1 percent or less) with projectile mass.

If the projectile base pressure versus distance curves were the same for various projectile masses for each case, the muzzle velocity would vary as the projectile mass to the -0.5 power. The reality is quite different. The lighter projectiles run away from the driving gas more rapidly, causing the projectile base pressures to fall below those for the heavier projectiles. This can be seen in Figs. 15 and 16. We see that, for the four P10 gun configurations, the exponents are significantly different for the different pump tube L/Ds. This is to be expected, since the shapes of the projectile base pressure versus time curves are quite different for the different L/Ds. (See Fig. 11.) For example, if one considers Fig. 11, the curves of which are for a projectile mass of 0.2167 g, and imagines the lighter 0.12989 g projectile running away more rapidly from the driving gas, the loss of driving pressure would be expected to be different due to the different shapes of the base pressure histories for the heavier projectile.

The above discussion gives a general feel for the effect of projectile mass on the muzzle velocity and the maximum projectile base pressure. However, as noted above, the details could be somewhat different for the gun operating conditions, e.g., for different pump tube L/Ds, piston masses and hydrogen pressures.

L. Break valve rupture pressure effect.

Two basic cases were studied. One was a P10 gun configuration, for the condition shown in Figs. 8 and 9 with a pump tube L/D of 36.4. The second was for the Ames HV gun for a condition similar to that shown in Figs. 5 – 8, but with somewhat lower powder loads such that the muzzle velocity was 9.80 km/sec rather than 10 km/sec. The effects of varying the break valve rupture pressure on the maximum gun pressures and the maximum projectile base pressures are shown by the green and light blue data points in Fig. 17. The effect of decreasing the break valve rupture pressure from 30 ksi to 20 ksi is seen to decrease the maximum projectile base pressure and to increase the maximum gun pressure. This is most likely due to the fact that if the break valve ruptures at a lower pressure, the piston will slowed down by the gas less and it will eventually jam into the high pressure coupling contraction cone with more force. We note that the percentage changes produced are different for the two basic cases studied. For the P10 gun case, the decrease in the maximum projectile base pressure is 12.3%, but for the Ames HV

gun, it is 8.3%. For the P10 gun case, the increase in the maximum gun pressure is 12.4%, but for the Ames HV gun, it is only 3.8%. Thus, the two basic cases studied to date give the direction of changes of the maximum pressures and the order of magnitude (4 – 12%) of the changes, but if details were required for other basic conditions, additional CFD calculations would be required.

M. Possible pump tube/launch tube diameter ratio effect.

This discussion begins with a presentation, in Table 9 below, of high velocity launch conditions for various guns. The nomenclature for the data is:

D – launch tube diameter
D_p – pump tube diameter
L_p – pump tube length
V_p – pump tube volume
m – projectile mass
v_{muz} – muzzle velocity
H_2 press – hydrogen pressure
m_g – mass of hydrogen gas

The data for the first seven guns shown in the table are taken or derived from the table of Ref. 9. For these seven guns, the shots shown are the highest velocity experimental shots. The shot of eighth gun shown is that for the optimized P10 gun of this report with a pump tube L/D of 36.4. This shot is only a calculated (CFD) shot. We note that the Ames HV gun shot of Table 9 is not at the same condition as that discussed earlier herein, which was presented, for example, in Figs. 5 – 8, with a muzzle velocity of 10.0 km/sec. The Ames HV gun shot of Table 9 is, instead, the highest muzzle velocity shot ever achieved with that gun with a very light projectile.

The diameter ratio D_p/D chosen for the P10 gun is in the middle of the range of values for the guns for the high velocity (>10.7 km/s) shots of Table 9, but it is somewhat higher than the average value (~4.7) for the Ames standard stable of guns. With our range of L/D values (27.3 to 153.3) for the P10 gun configurations studied, we have covered the range of V_p/D^3 values of 4230 to 23,750 but have not actually varied D_p/D. It would seem unlikely that substantial improvements could be obtained if D_p/D were to be varied, but such studies have not been made to date.

Table 9. Guns and gun operating conditions for various high velocity shots.

Gun	D_p/D	L_p/D_p	V_p/D^3	m/D^3 (g/cm^3)	v_{muz} (km/s)	H_2 press (psia)	m_g/m
*Ames 0.28”/1.55”	5.53	273	36,260	0.452	9.24	7.24	3.36
*Ames 0.50”/2.54”	5.07	246	25,180	0.459	9.46	10	3.12
*Ames 1.0”/4.0”	4.00	244	12,260	0.453	8.44	30	4.65
*Ames 1.5”/6.23”	4.15	208	11,680	0.275	9.07	30	4.05
Ames 0.22”/1.28” (HV)	5.82	115	17,810	0.260	11.3	40	15.6
Ames 0.22”/1.77”	8.04	93	37,960	0.298	10.84	23	16.76
GM 0.22”/1.00”	4.53	145	10,590	0.305	10.8	58	11.61
P10 0.313”/1.82”	5.82	36.4	5,640	0.433	10.0	346	25.33

*Ames standard stable of guns

N. Presentation of the optimized P10 gun with pump tube L/D of 36.4

Figure 18 shows the P10 gun configuration with a pump tube L/D of 36.4 and gives the gun dimensions. Key gun parameters are listed below:

Launch tube diameter (D) = 0.3125" = 0.7938 cm
Pump tube diameter (D_p) = 1.818" = 4.6195 cm
D_p/D – 5.818
Pump tube L/D – 36.4
Powder – IMR 4320
Powder mass – 798.9 g
Piston mass – 286.6 g
Hydrogen pressure – 346 psia
Break valve rupture pressure – 27.5 ksi
Projectile mass – 0.2187 g
Piston velocity (between whisker gauges shown in Fig. 16) – 845.4 m/s
Muzzle velocity – 10.0 km/s
Maximum gun pressure – 1.946×10^{10} dy/cm^2 = 282 ksi
Maximum projectile base pressure – 2.346×10^9 dy/cm^2 = 34 ksi

As mentioned earlier (see Sec. G), it is the author's opinion that L/D = 36.4 is a good candidate to be the optimum pump tube length for the P10 gun. For reference, Table 10 below gives key operating parameters for all seven optimized P10 guns for which data is shown in Figs. 5 – 9. The geometries of all the P10 guns can be constructed from the geometry shown in Fig. 18 by adding the length change from Table 10 to all dimensions to the right of line AA in Fig. 18.

The powder burn rate equation used in the present CFD calculations is that "tuned" to match the measured powder pressure burn histories for a particular shot in the Ames 0.5" gun.[10,11] With this "tuned" powder burn rate, the experimental and measured maximum powder chamber pressures were found to agree well for 14 different shots with maximum powder chamber pressures ranging from 4.5×10^8 to 1.1×10^9 dy/cm^2 (Ref. 12). To obtain this good agreement, it was found that the burn rate equation provided by DuPont[6] had to be multiplied by a factor of 1.64. For the P10 optimized guns with pump tube L/Ds of 36.4 and 27.3, the maximum powder chamber pressures are 1.4×10^9 and 2.0×10^9 dy/cm^2, respectively. These are outside the range of the good agreement of the "tuned" burn rate equation discussed in Refs. 10 and 12. For this reason and, also, as a general principle, the powder load given above for the P10 optimized gun

Table 10. Gun parameters for seven optimized P10 guns.

Pump tube L/D	Powder mass (g)	Piston mass (g)	Hydrogen pressure (psia)	Piston velocity (m/s)	Length change from L/D = 36.4 case (cm)
153.3	209.2	215	24.18	925.9	528.30
115	236.4	215	32.24	890.6	355.13
86.3	272.3	215	46.19	860.3	225.25
64.7	434.2	286.6	109.5	878.5	127.85
48.5	642.0	286.6	224.8	910.6	54.79
36.4	798.9	286.6	346.0	845.4	0.0
27.3	1043.2	286.6	532.7	777.4	-41.09

configuration with pump tube L/D = 36.4 cannot be taken as exact, but only as a reasonable starting point. Rather, the powder load should be adjusted so that the experimental piston velocity matches the piston velocity of the CFD calculations. This should result in a gun operating condition close to that given in the table. This also applies for the powder loads of the guns listed in Table 10.

O. Possibilities for velocities above 10 km/s – lighter projectiles, increased powder loads.

As already discussed in the section on the projectile mass effect (Sec. K, Figs. 15 and 16), with lighter projectiles, higher muzzle velocities can be achieved. Higher muzzle velocities can also be achieved by increasing the powder loads. We start with the optimized P10 gun condition for a pump tube L/D = 36.4 which was studied in detail previously. This P10 gun condition, like all seven of the optimized P10 gun conditions studied previously, is for a muzzle velocity of 10 km/sec. CFD calculations were made for three different projectile masses and 11 or 12 different powder loads. These masses were 0.2465, 0.2167 and 0.1298 g, which correspond to normalized masses [(projectile mass)/(launch tube diameter)^3] of 0.4929, 0.4333 and 0.2596 g/cm^3, respectively. The results are shown in Figs. 19 – 21. Figures 19, 20 and 21 show, respectively, the maximum gun pressures, maximum projectile base pressures and powder masses as functions of the muzzle velocity. The optimized condition for L/D = 36.4 and a muzzle velocity of 10 km/sec is indicated by the arrow in each figure.

The velocities which can practically be achieved depend upon not exceeding the pressure limits of the gun or the launch package. For a slug (simple cylinder) projectile, these were estimated as follows. Shot number 20-80 (6/8/66) of the Ames 0.5” gun was modeled with the CFD. This is the highest velocity shot made with this gun. The experimental muzzle velocity was 9.46 km/sec and the CFD value was 9.41 km/sec, a difference of 0.6%. Subsequent to this shot, twelve more shots were made over a 3 week period, with 4 shots between 9.15 and 9.42 km/sec and single shots at 8.11 and 8.86 km/sec. (Some of the shots were with much heavier projectiles at muzzle velocities of 4.9 to 6.7 km/sec.) Thus, there was no indication that shot 20-80 damaged the gun. Then, a shot (shot 33-93) was made at an increased powder load and at the minimum hydrogen pressure (10 psia). This last shot destroyed the high pressure coupling (HPC) of the gun and the projectile. We take the CFD calculated maximum pressures for shot 20-80 as the limiting pressures. These are 0.339 x 10^{11} dy/cm^2 for the maximum gun pressure and 0.535 x 10^{10} dy/cm^2 for the maximum projectile base pressures. These pressure limits are shown as dashed lines in Figs. 19 and 20, respectively. (We note that the CFD calculated maximum gun pressure for shot 33-93, which destroyed the HPC, was 0.769 x 10^{11} dy/cm^2, about 2.3 times the CFD value for the successful shot.)

The limit for the projectile base pressure given above is assumed to apply for slug (simple cylinder) models, which are subject to hydrostatic type acceleration loads. This limit would not be expected to apply to a launch package consisting of a sphere in a sabot, which is subject to acceleration loads very different than hydrostatic, in that the denser sphere can “fall through” the lighter sabot material, “cookie-cutting” out the center part of the rear of the sabot. A representative such sabot is shown in Fig. 22 (taken from Ref. 13). The aluminum sphere of Fig. 22 was launched, using a Nylon sabot, at 9.4 km/sec. The launch package mass for this shot was 0.0860 g. The maximum projectile base pressure for this shot was estimated as follows. The launch gun for this shot is not mentioned in Ref. 13, but since the shot was performed at the Ames Research Center with a 0.22” caliber gun, we have assumed that the launch gun was the Ames HV (1.28”/0.22”) gun discussed previously, for example, in Sec. IIA. The operating conditions for the Ames HV gun for this 9.4 km/sec shot were obtained by taking the conditions for the Ames HV gun shot of Table 9, changing the projectile mass from 0.0756 to 0.0860 g and adjusting the powder load to produce the 9.4 km/sec muzzle velocity. This resulted in a

maximum projectile base pressure of 0.4092 x 10^{10} dy/cm^2 for a saboted sphere, a limit which is considerably less than the limiting value of 0.5348 x 10^{10} dy/cm^2 estimated earlier for a simple slug projectile. This lower limit is shown as a dashed line in Fig. 20.

For slug projectiles, the maximum gun pressure shown in Fig. 19 is limiting. This would result in maximum muzzle velocities of 10.30, 10.47 and 11.05 km/sec for the curves for the three projectile masses shown in Fig. 19. For the saboted sphere (with a launch mass of 0.2465 g) (see Fig. 20), the maximum projectile base pressure is limiting and results in a maximum muzzle velocity of 10.25 km/sec. For the saboted sphere of Fig. 22, the ratio of sphere diameter to launch tube diameter is 0.286. In Ref. 14, launch of an aluminum sphere to a velocity of 9.89 km/s is reported. For this launch, the ratio of sphere diameter to launch tube diameter was 0.188. Based on the sabot of Fig. 22, the concept of a sabot design for the smaller sphere shown in Fig. 23 was developed. The thickness of sabot material underneath the sphere divided by the sphere diameter is the same for the sabots of Figs. 22 and 23. The estimated mass of the launch package of Fig. 23, scaled to the size of the P10 guns, is 0.1785 g. (It is to be emphasized that the sabot design of Fig. 23 is conceptual only and has not been proven.) In Fig. 20, an estimated curve for a projectile mass of 0.1785 g has been sketched in. (Nearly the same location for the estimated curve is obtained no matter which two curves for which we have actual calculations are used.) If the sabot of Fig. 23 could, in fact, survive the maximum base pressures that were calculated above for the sabot of Fig. 22, it would seem that for small saboted spheres, successful launches may be possible at muzzle velocities of 10.7 – 10.8 km/s. Such predicted high performances must, of course, be verified in the ballistic range. It should be noted that the pressure limits calculated above are estimated for launches in which both the projectile and gun have survived and are not absolute limits. It may be possible to surpass these limits slightly, but we note that the pressure curves rise very steeply with increasing muzzle velocity and it is the author's opinion that these limits cannot be substantially exceeded.

From the above discussion, it appears that saboted projectiles of various materials could be launched at velocities of 10.25 and possibly as high as 10.8 km/s, but that launches at the highest velocities of 11.05 km/s would be restricted to small L/D disc-like plastic models. With the low mass launch packages required for the 11 km/s range it would appear to be very difficult to obtain sufficient sabot support material beneath, say, a small denser sphere projectile to prevent it from "falling through" the sabot under the launch accelerations.

P. Possibilities for velocities above 10 km/s – refractory metal barrel liners or coatings.

Reference 3 presents CFD calculations of two-stage light gas internal ballistics showing that, at higher muzzle velocities (above ~7 km/sec), substantial quantities of steel are eroded from the bore of the gun. This eroded steel is then incorporated into the hydrogen working gas of the gun. This can significantly load down the working gas so that the muzzle velocities achievable are substantially reduced. At (actual) muzzle velocities of 8 – 9.5 km/s, the losses of muzzle velocity due to loading of the hydrogen working gas with steel can be 2 to 4 km/s. This is to say that, at actual muzzle velocities of 8 to 9.5 km/s, if there were no loading down of the hydrogen with eroded gun tube material, muzzle velocities of 10 to 13 km/s would be achievable.

Reference 15 presents CFD calculations of a two-stage light gas gun with rhenium instead of steel gun tubes. For 16 of the 17 cases studied, this change of gun tube material reduced the bore erosion to zero, with the result that muzzle velocities of 9 to as high as 13 km/sec were predicted with the rhenium liner. In Ref. 15, Tantalum and molybdenum were discarded due to inferior thermal properties and yield strengths. Based on other considerations not taken into account when Ref. 15 was written, discarding tantalum must now be regarded as incorrect. The metals with the highest melting points are rhenium (Re), tantalum (Ta) and tungsten (W). Table 11 gives relevant properties of these metals plus those of a Ta – 10% W alloy which has been used

as a gun barrel liner. Also given are data for gun steel, which is typically AISI 4340 steel. The data of Table 11 were taken from Refs. 16 – 18 and the property values are at room temperature. The refractory metals are very expensive and therefore must be used as liners or coatings in gun tubes, with the main material of the gun tube usually being gun steel. In Ref. 19, the effect of the elastic modulus of the liner/coating materials is discussed. It is pointed out that those liner/coating materials with moduli greater than that of the gun steel jacket do not effectively transfer the load to the jacket material and are prone to cracking. By contrast, those liner/jacket materials with moduli less than that of the jacket, especially if they are ductile, effectively transfer the load to the jacket and are not prone to cracking.

Table 11. Key properties of potential materials for gun barrel liners or coatings.

Metal	Re	Ta	Ta-10W	W	Gun steel
Modulus of elasticity, Msi	68	27	29	59	30
Tensile strength, ksi	280	60	160	220	
Reduction of area, %	35	95+	85+	0	
Melting point, K	3456	3269	3320	3683	1723
Density, g/cm^3	21.0	16.6		19.2	7.80
Thermal conductivity, W/m/K	75.6	54.5		167.1	43
Specific heat, kJ/kg/K	0.147	0.151		0.142	0.473

Tantalum and Ta-10W and similar alloys have been used as liners and coatings in military powder guns and have been shown to be effective in reducing gun barrel erosion. Reference 20 discusses the use Ta-10W and T222 alloy (Ta-10W-2.5Hf-0.01C) liners in a 7.62 mm gun system to reduce erosion. (Other liner materials were also discussed in Ref. 20.) References 21 – 23 discuss the use of tantalum coatings over steel in a 20 mm gun system and very encouraging results were obtained. Based on the discussion of the preceding paragraph and the successful implementation of tantalum and tantalum alloy liners/coatings discussed in Refs. 21 – 23, it is apparent that tantalum would be the material of choice for the liner/coating for a two-stage light gas gun.

However, from Table 11, it is seen that the thermal properties of tantalum are somewhat inferior to those of rhenium, in that the melting point, density and thermal conductivity of Ta are lower than the corresponding values for Re. Hence, to verify the suitability of tantalum as a liner material for two stage light gas guns, CFD calculations of high muzzle velocity shots were performed with tantalum, rhenium and steel gun tubes.[24] Muzzle velocities for the three types of gun tube material were presented in the reference. It was shown that, with the exception of the highest velocity shot modeled, the muzzle velocity gains with tantalum tubes (when compared with steel tubes) are very nearly the same as those achievable with rhenium tubes. Even for the highest velocity shot, the tantalum/steel velocity gain is 82% that of the rhenium/steel velocity gain. For all except the highest velocity shot, the gun erosion with tantalum tubes ranged from 0 to 14% of that with steel tubes to be compared with 0 to 5% for rhenium tubes. Thus, the CFD calculations of Ref. 24 confirm the suitability of tantalum as a liner material for two stage light gas guns.

III. SUMMARY AND CONCLUSIONS

The design of a two-stage light gas gun for muzzle velocities of 10 to 11 km/s for space debris impact studies was studied. The gun design starts with a 0.22”/1.28” gun at the NASA Ames Research Center which has achieved muzzle velocities of 10 – 11 km/s. The gun was scaled up to a launch tube diameter of 0.3125”. For the original pump tube L/D of 115, the gun

was optimized with respect to maximum pressures for hydrogen pressure and piston mass. The optimization was then repeated for six other pump tube L/Ds ranging from 153.3 down to 27.3. A pump tube L/D of 36.4 was selected giving the best overall performance and further studies focused on this L/D value. Piezometric ratios were presented and it was shown that, for the lower pump tube L/Ds of 48.5 to 27.3 and high hydrogen changing pressures, the piezometric ratios are ~2.3, comparable to those for military powder guns. The more traditional two stage light gas guns at Ames, with pump tube L/Ds of 210 to 270 and much lower hydrogen charging pressures, produce piezometric ratios typically of 4 to 6, much less favorable. For an optimized gun with pump tube L/D of 36.4, the maximum pressures at all locations along the gun were presented. For all seven pump tube L/Ds for the optimized guns, the maximum powder chamber pressures were presented. The maximum pressures were 20 to 30 ksi, to be compared with values of 40 to 60 ksi for high performance military systems.

The effect of varying the included angle of the cone of the high pressure coupling on the maximum pressures was studied and it was concluded that desirable range of angles was 7.3 to 14.6 degrees to minimize the maximum pressures. The effect of varying the projectile mass was studied and it was found that reducing the projectile mass by a factor of 1.67 increased muzzle velocities from 10 km/s up to 10.5 to 10.9 km/s and decreased the maximum projectile base pressures by factors of 1.3 to 1.6. The effect of varying the break valve rupture pressures was studied and it was concluded that lowering the rupture pressure lowered the maximum projectile base pressure, but raised the maximum gun pressure. The possible effect of varying the pump tube diameter was discussed, but no actual CFD study calculations were performed. The key gun operating parameters for optimized guns with all seven pump tube L/Ds were presented along with a sketch for the optimized gun with L/D = 36.4.

For the optimized gun with a pump tube L/D of 36.4, increasing the muzzle velocity by decreasing the projectile mass and increasing the powder loads were studied. Pressure limits for the gun, a slug projectile and a saboted sphere projectile were established. It appears that saboted spheres could be launched to 10.25 km/s and possibly as high as 10.8 km/sec, and that disc-like plastic models could be launched to 11.05 km/s. The use of refractory metal liners to minimize loading down the hydrogen working gas with eroded gun tube wall material and thus limiting the muzzle velocity, was discussed. Tantalum was established as the liner material of choice. With a tantalum liner, CFD code calculations of Ref. 24 predict muzzle velocities as high as 12 to 13 km/s.

The goal of the present study is to obtain higher velocity launches of projectiles of known shapes. If this is achievable in practice, it would permit better simulation of space debris impacts.

ACKNOWLEDGEMENT

Support by NASA (Contract NNA15BB15C) to Analytical Mechanics Associates, Inc. is gratefully acknowledged.

REFERENCES

1. Bogdanoff, D. W., “New Higher-Order Godunov Code for Modelling Performance of Two-Stage Light Gas Guns,” NASA TM 110363, September, 1995.
2. Bogdanoff, D. W., “CFD Modelling of Bore Erosion in Two-Stage Light Gas Guns,” NASA TM-1998-112236, August, 1998.
3. Canning, T. N., Seiff, A. and James, C. S., “Ballistic Range Technology,” AGARDograph

138, published by the North Atlantic Treaty Organization, Advisory Group for Aerospace Research and Development (AGARD), August, 1970, p. 58.
4. Denardo, B. P., "Penetration of Polyethylene into Semi-Infinite 2024-T351 Aluminum up to Velocities of 37,000 Feet per Second," NASA TN D3369, March, 1966.
5. Curtis, J. S., "An Accelerated Reservoir Light-Gas Gun," NASA TN D-1144, February, 1962.
6. E. I. DuPont de Nemours & Co., Inc., "Smokeless Powder Technical - Properties of DuPont IMR powders."
7. Bogdanoff, D. W., "New Higher-Order Godunov Code for Modelling Performance of Two-Stage Light Gas Guns," NASA TM 110363, September, 1995, p. 33, Fig. 23.
8. Steifel, L., ed., "Gun Propulsion Technology," Vol. 109, Progress in Astronautics and Aeronautics series, published by the American Institute of Aeronautics and Astronautics, 1988, pp. 61 – 74.
9. Canning, T. N., Seiff, A. and James, C. S., op. cit., p. 58.
10. Bogdanoff, D. W., op. cit., pp. 9 – 12.
11. Bogdanoff, D. W., op. cit., pp. 21 – 23.
12. Bogdanoff, D. W., "CFD Modelling of Bore Erosion in Two-Stage Light Gas Guns," NASA TM-1998-112236, August, 1998, p. 27.
13. Canning, T. N., Seiff, A. and James, C. S., op. cit., Fig. 3.42, p. 149.
14. Piekutowski, A. J., Poormon, K. L., Christiansen, E. L. and Davis, B. A., "Performance of Whipple Shields at Impact Velocities above 9 km/s," *International Journal of Impact Engineering*, Vol. 38, 2011, pp. 495 – 503.For
15. Bogdanoff, D. W., "Use of a Rhenium Liner to Reduce Bore Erosion in Two-Stage Light Gas Guns," presented at the 50th Meeting of the Aeroballistic Range Association, Pleasanton, California, November 8 – 12, 1999.
16. Steifel, L., ed., op. cit., p. 315.
17. *Machine Design*, December 1993, pp. 33, 90, 91.
18. Holman, J. P., "Heat Transfer," 6th ed., McGraw-Hill, New York, 1986, p. 635.
19. Steifel, L., ed., op. cit., p. 339-340.
20. ibid, pp. 338-339.
21. ibid, pp. 347.
22. Ahmad, I., Barranco, J., Aalto, P. and Cox, J., "Studies of Refractory Metal Coatings for Advanced Gun Barrels," US Army Armament Research and Development Center, Benet Weapons Laboratory, Watervliet, NY, Technical Report ARLCB-TR-83029, July, 1983, especially pp. 40-47.
23. Cullinan, R., D'Andrea, G., Croteau, P. and Arnold, C., "Study of Erosion Resistant Materials for Gun Tubes: Part I, 20 mm Technology," US Army Armament Research and Development Center, Benet Weapons Laboratory, Watervliet, NY, Technical Report ARLCB-TR-80027, December 1980, especially pp. 96-97 (summary).
24. Bogdanoff, D. W., "Use of a Tantalum Liner to Reduce Bore Erosion and Increase Muzzle Velocity in Two-Stage Light Gas Guns," presented at the 66th Meeting of the Aeroballistic Range Association, San Antonio, Texas, October 4 – 9, 2015.

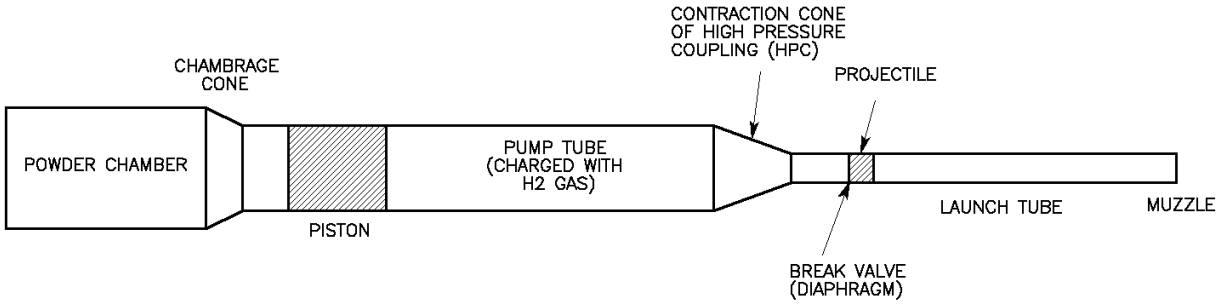

Fig. 1. Sketch of representative configuration of a two stage light gas gun. Not to scale.

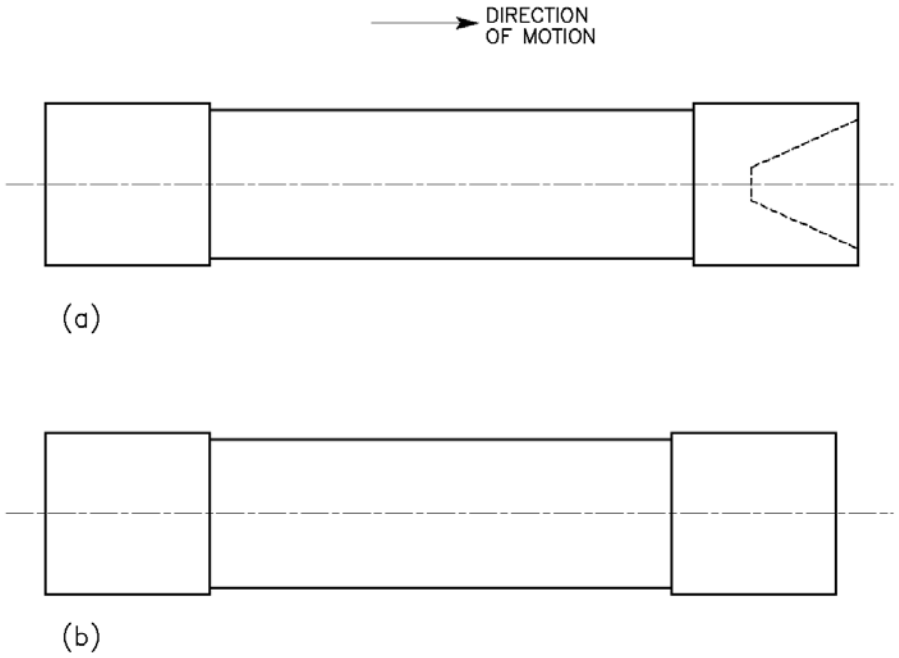

Fig. 2. Pistons for two stage light gas gun. (a), actual piston and (b), one-dimensional piston. Not to scale.

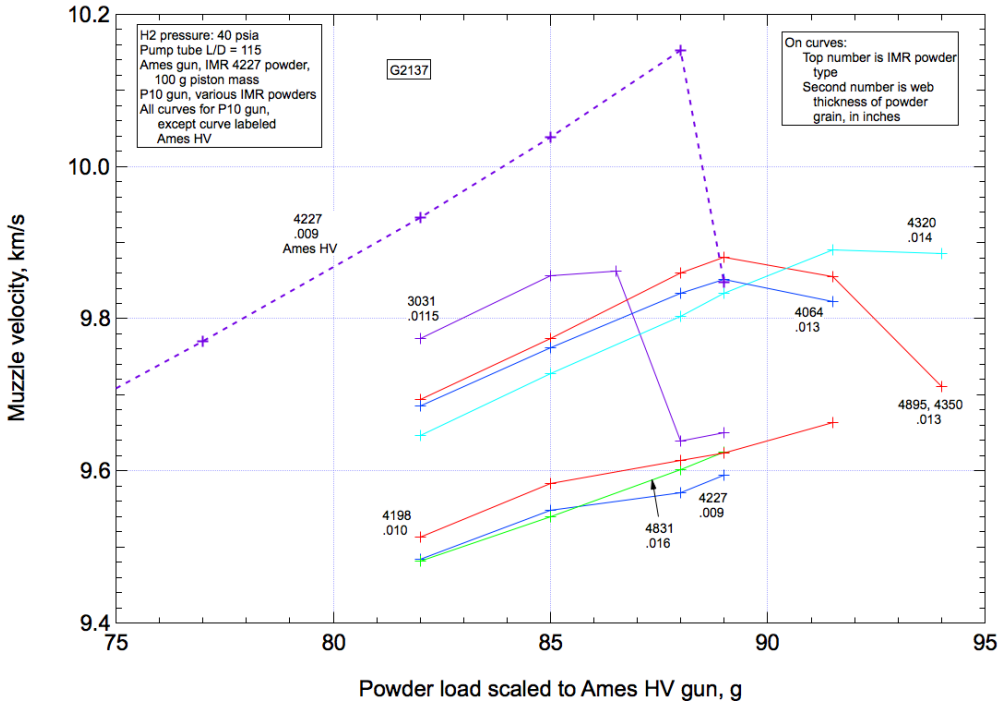

Fig. 3. Muzzle velocities for the Ames HV and P10 guns versus the normalized powder load for various IMR powders.

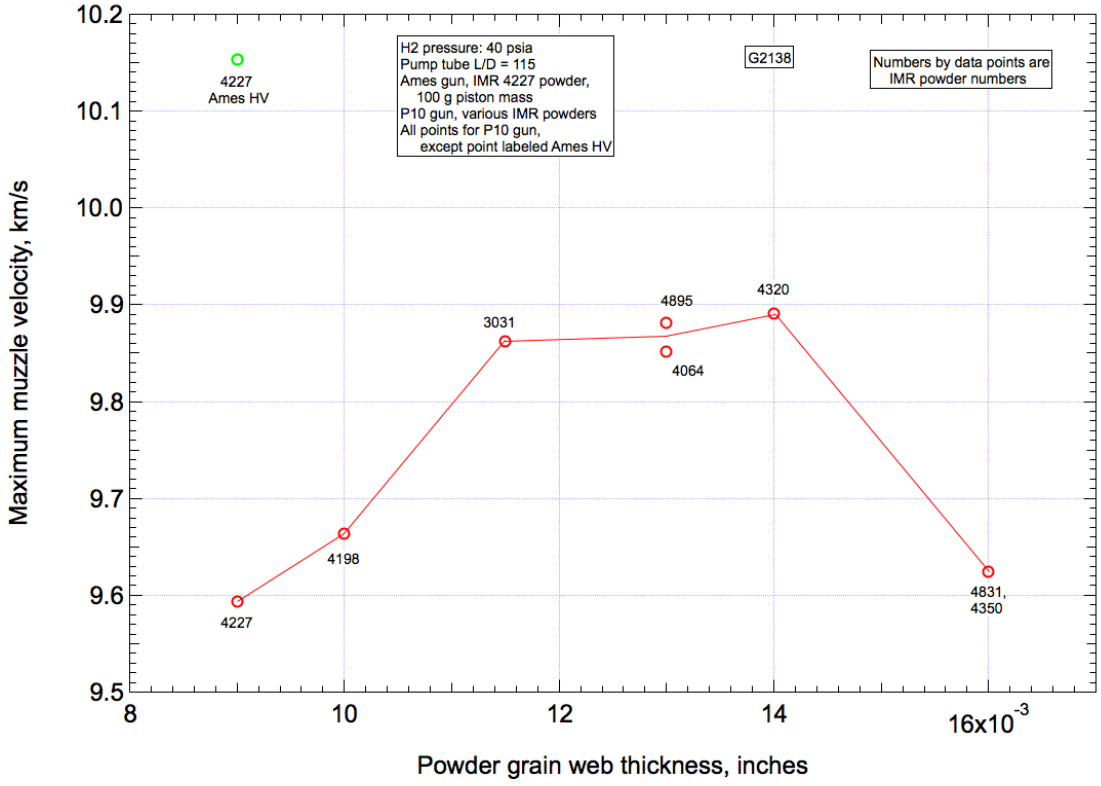

Fig. 4. Maximum muzzle velocities for the Ames HV and P10 guns versus the powder grain web size for various IMR powders.

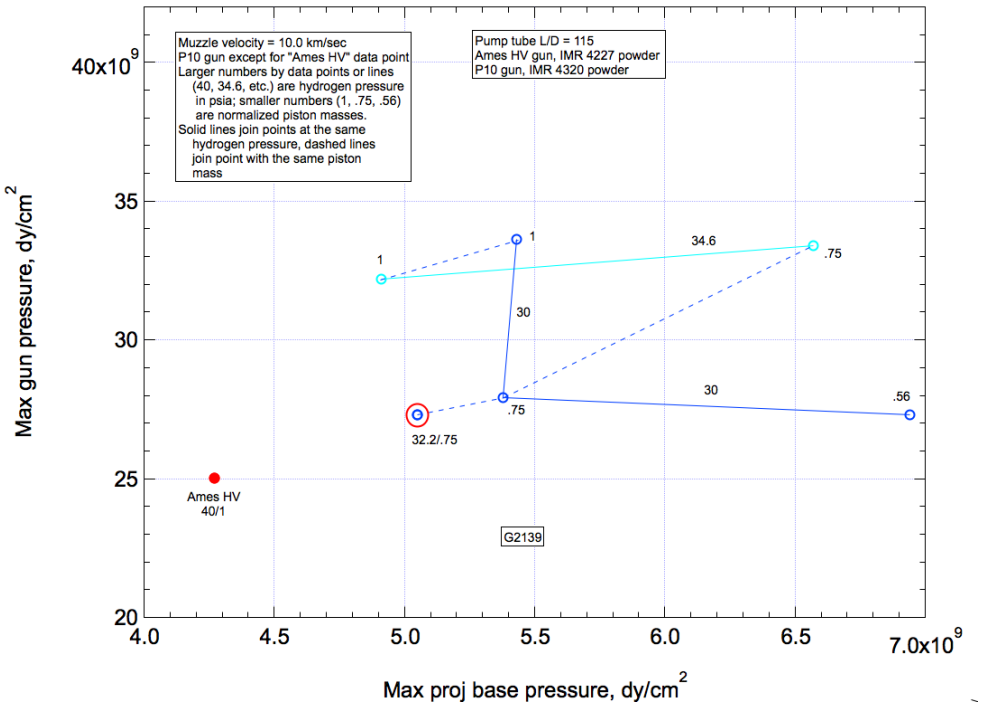

Fig. 5. Maximum model base pressures and maximum gun pressures for the P10 guns with a pump tube L/D of 115 for various hydrogen pressures and piston masses. Also shown is the data point for the Ames HV gun. Muzzle velocities are 10 km/s.

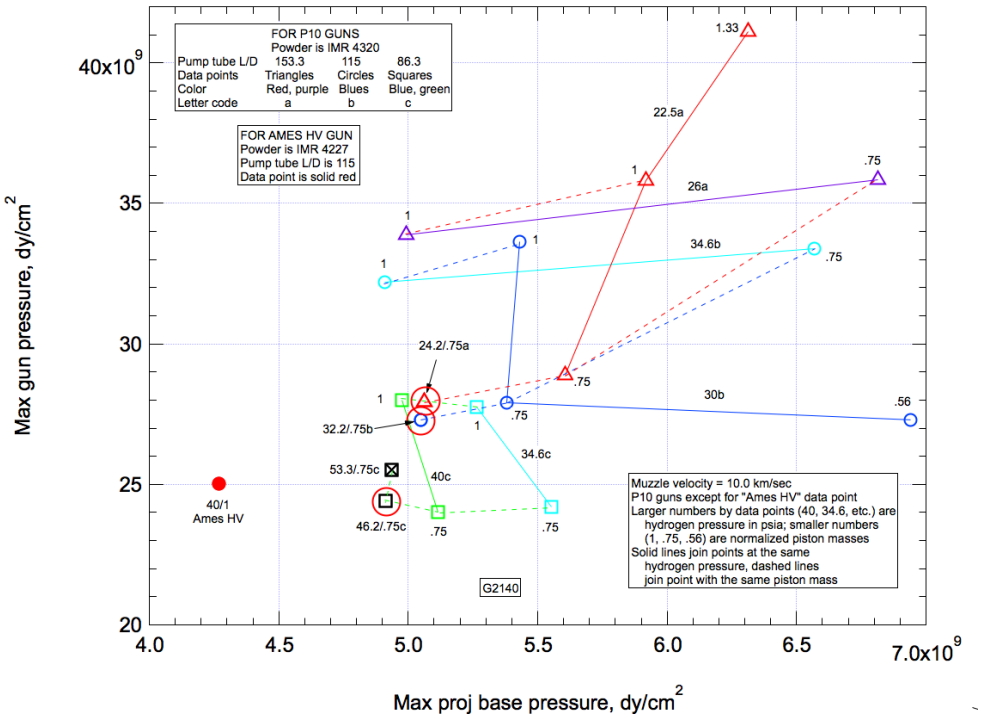

Fig. 6. Maximum model base pressures and maximum gun pressures for the P10 guns with pump tube L/Ds of 153.3, 115 and 86.3 for various hydrogen pressures and piston masses. Also shown is the data point for the Ames HV gun. Muzzle velocities are 10 km/s.

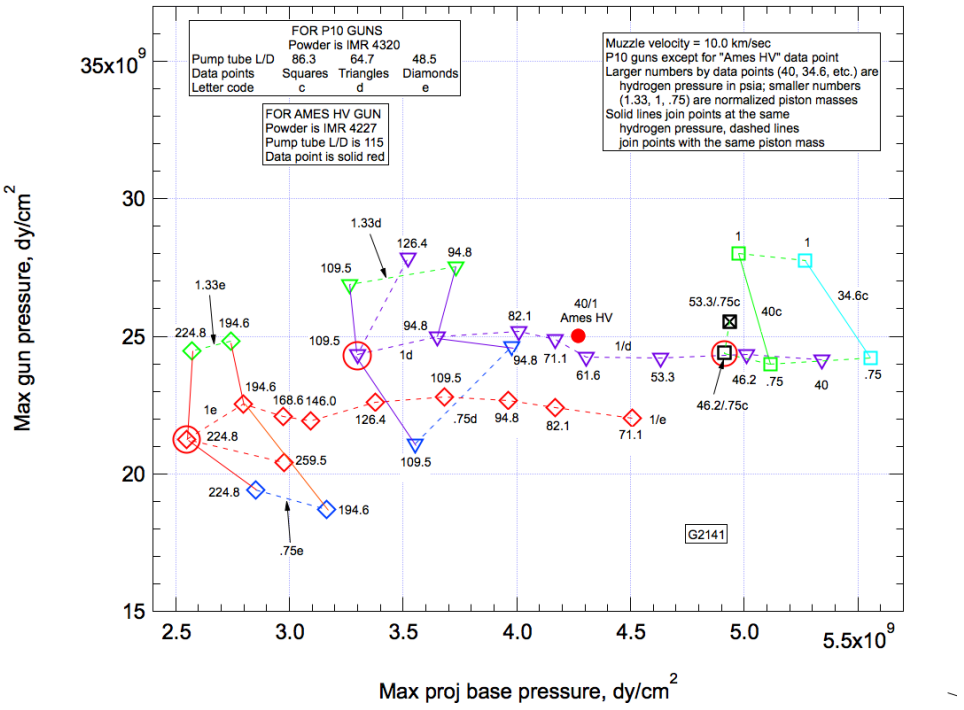

Fig. 7. Maximum model base pressures and maximum gun pressures for the P10 guns with pump tube L/Ds of 86.3, 64.7 and 48.5 for various hydrogen pressures and piston masses. Also shown is the data point for the Ames HV gun. Muzzle velocities are 10 km/s.

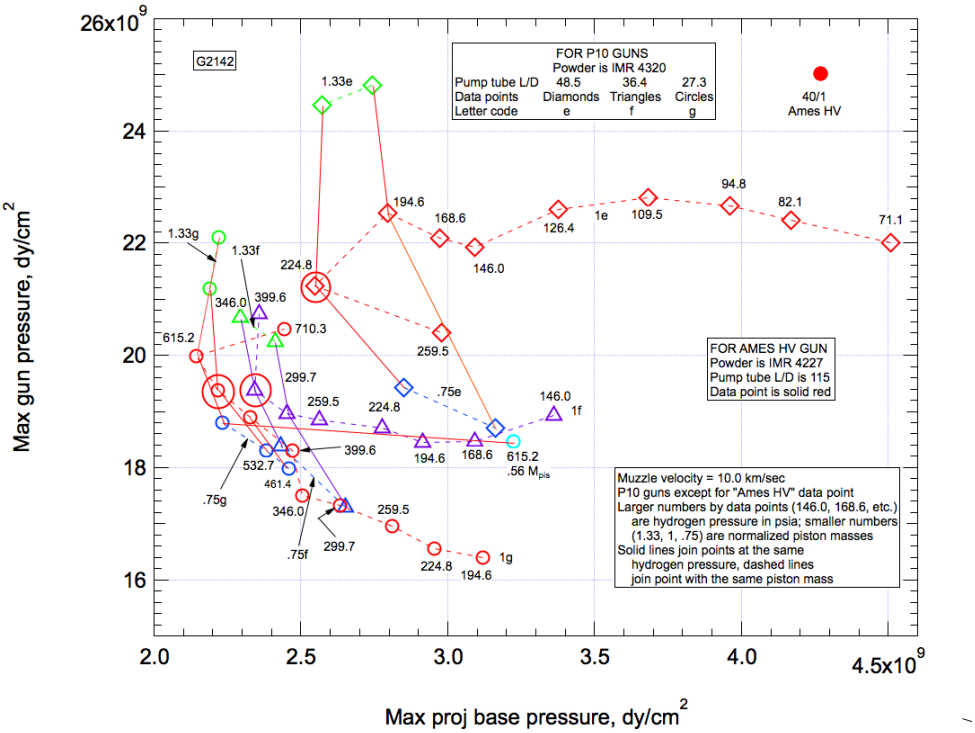

Fig. 8. Maximum model base pressures and maximum gun pressures for the P10 guns with pump tube L/Ds of 48.5, 36.4 and 27.3 for various hydrogen pressures and piston masses. Also shown is the data point for the Ames HV gun. Muzzle velocities are 10 km/s.

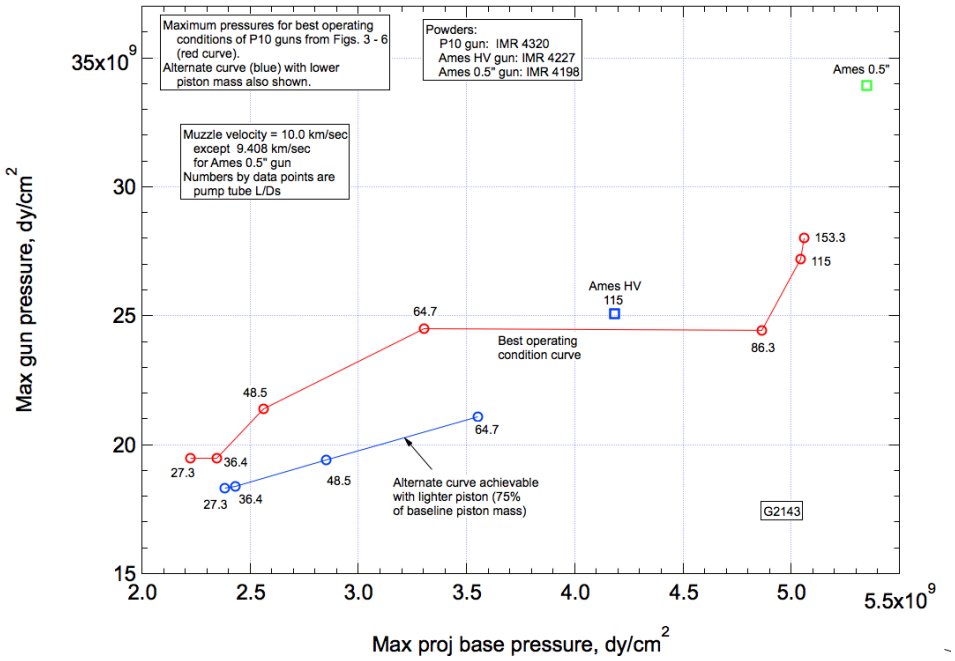

Fig. 9. Maximum model base pressures and maximum gun pressures for the optimum operating conditions for the P10 guns at 10 km/s for all pump tube L/Ds for the Ames HV gun at a muzzle velocity of 10 km/sec and the Ames 0.5" gun at a muzzle velocity of 9.408 km/sec. Also shown is an alternate curve of conditions achievable with a piston with a mass 75% of the baseline piston mass.

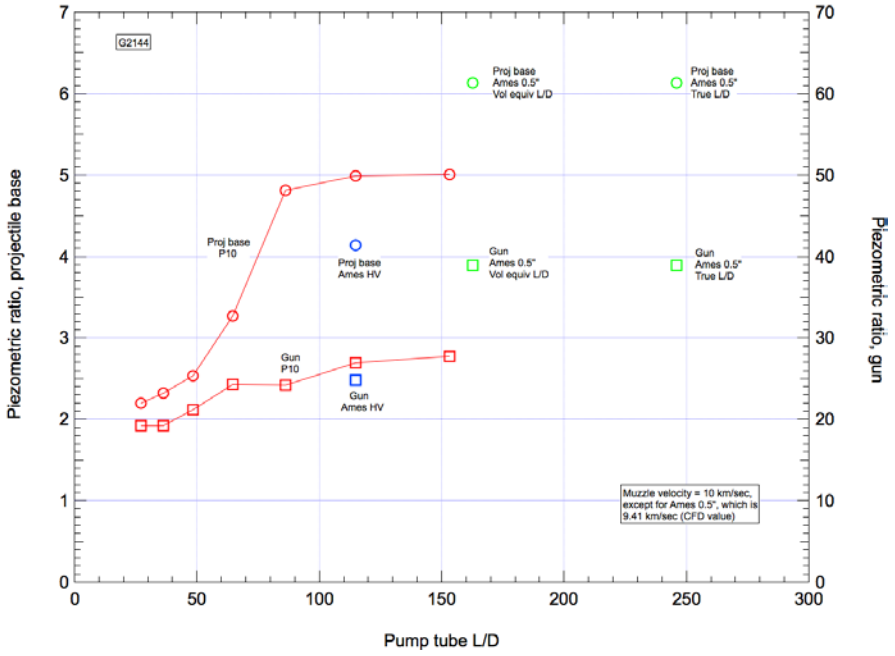

Fig. 10. Piezometric ratios for P10 and Ames guns plotted versus pump tube L/D values. "Proj" values (left side scale) are the conventional piezometric ratios, "Gun" values (right side scale) are a non-conventional piezometric ratio based on the maximum pressure at any location in the gun. See Sec. IIH for discussion of "Vol equiv L/D" and "True L/D".

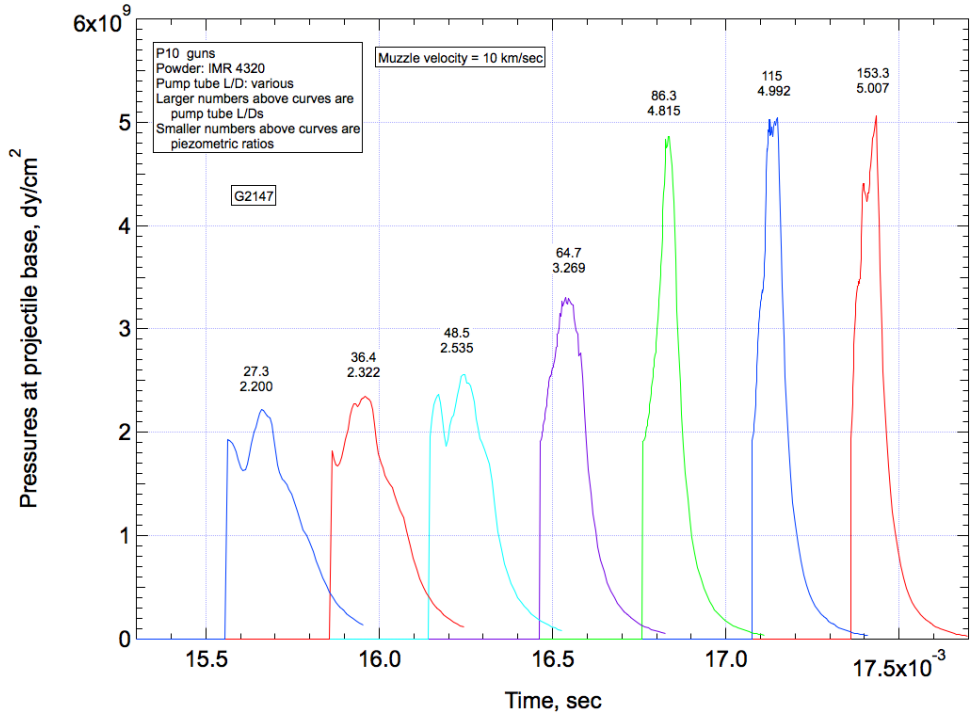

Fig. 11. Pressure histories at the projectile base for P10 guns for all pump tube L/Ds. L/Ds and piezometric ratios are shown above curves. Note that time origins have been shifted by arbitrary amounts to allow all curves to be shown on one plot.

.

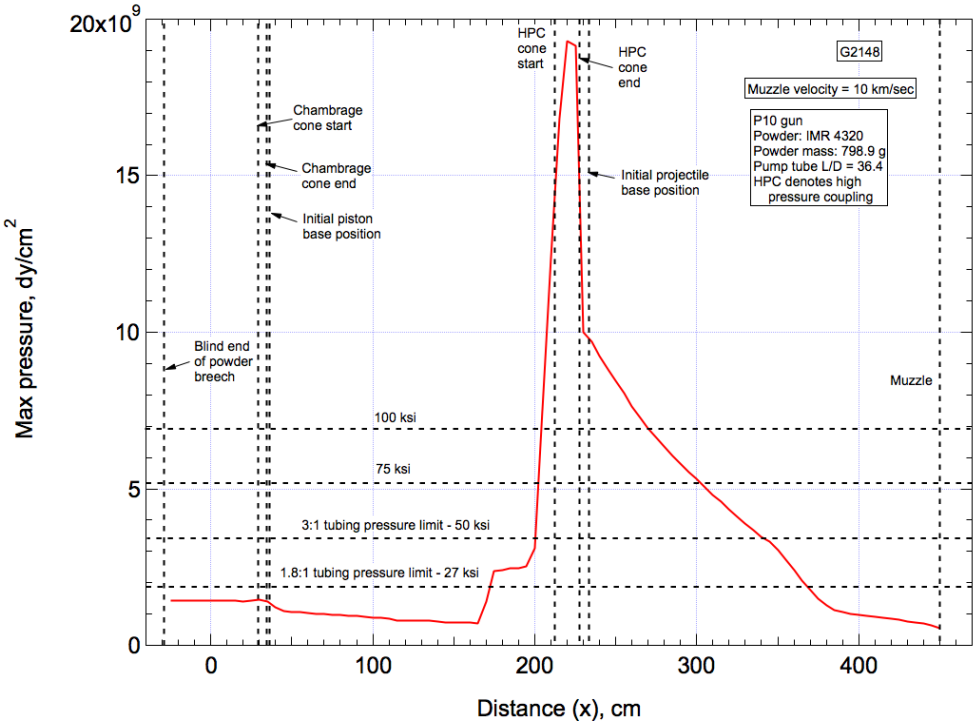

Figure 12. Maximum pressures reached at any time in the gun firing cycle plotted versus distance along the gun. For P10 gun with pump tube L/D = 36.4.

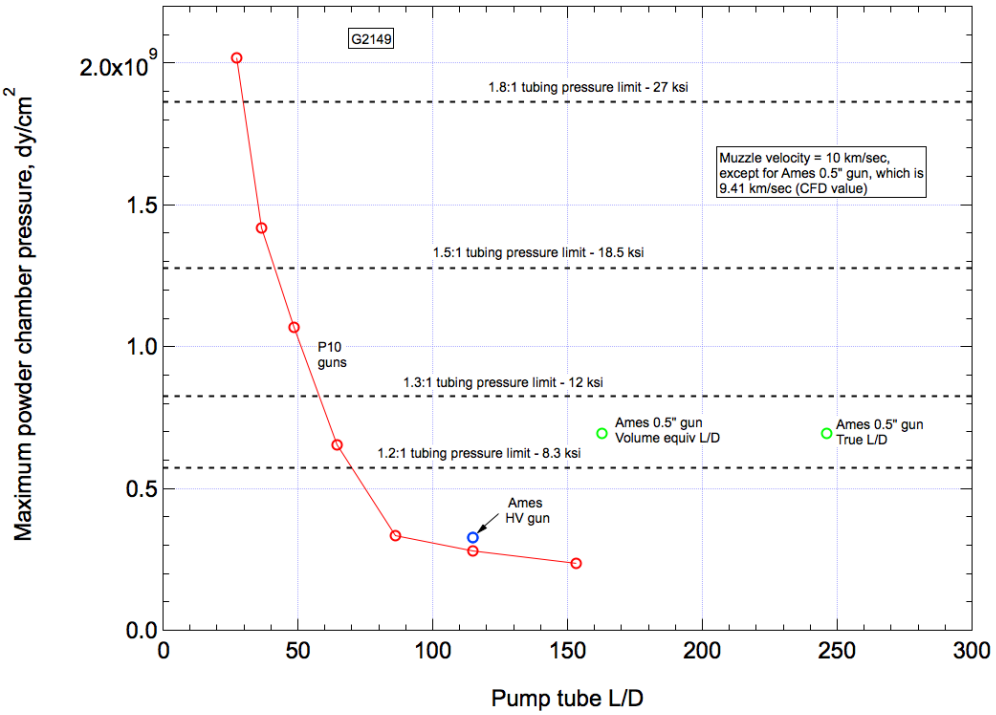

Fig. 13. Maximum powder chamber pressures for the P10 guns plotted versus pump tube L/Ds. Also shown are the CFD points for the Ames HV gun and the Ames 0.5" gun. See section IIH for discussion of "Vol equiv L/D" and "True L/D".

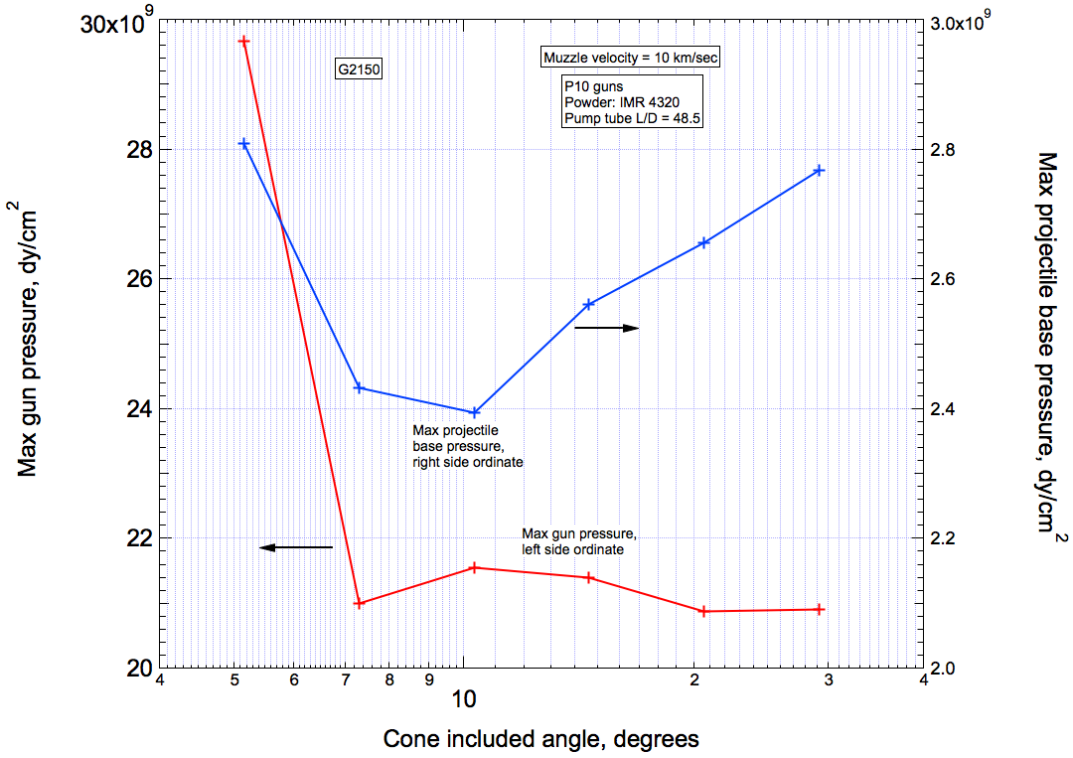

Fig. 14. Maximum gun pressures and maximum projectile base pressures for the P10 gun with pump tube L/D = 48.5 plotted versus the high pressure coupling contraction cone included angle.

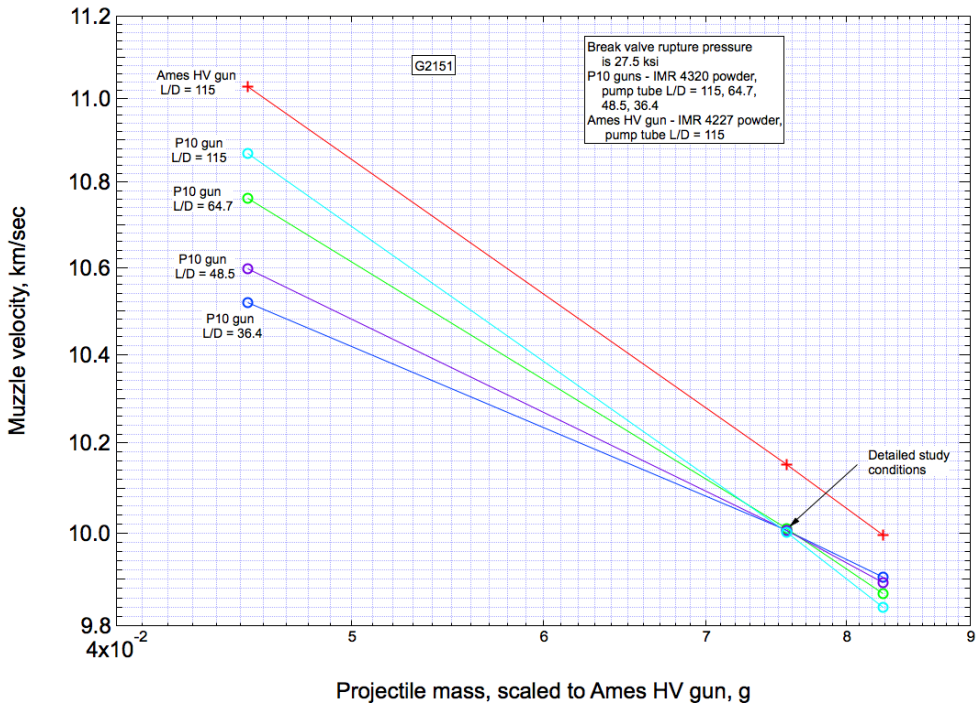

Fig. 15. Muzzle velocities versus projectile mass for the P10 gun configurations with pump tube L/Ds of 115, 64.7, 48.5 and 36.4 and for the Ames HV gun for a break valve rupture pressure of 27.5 ksi.

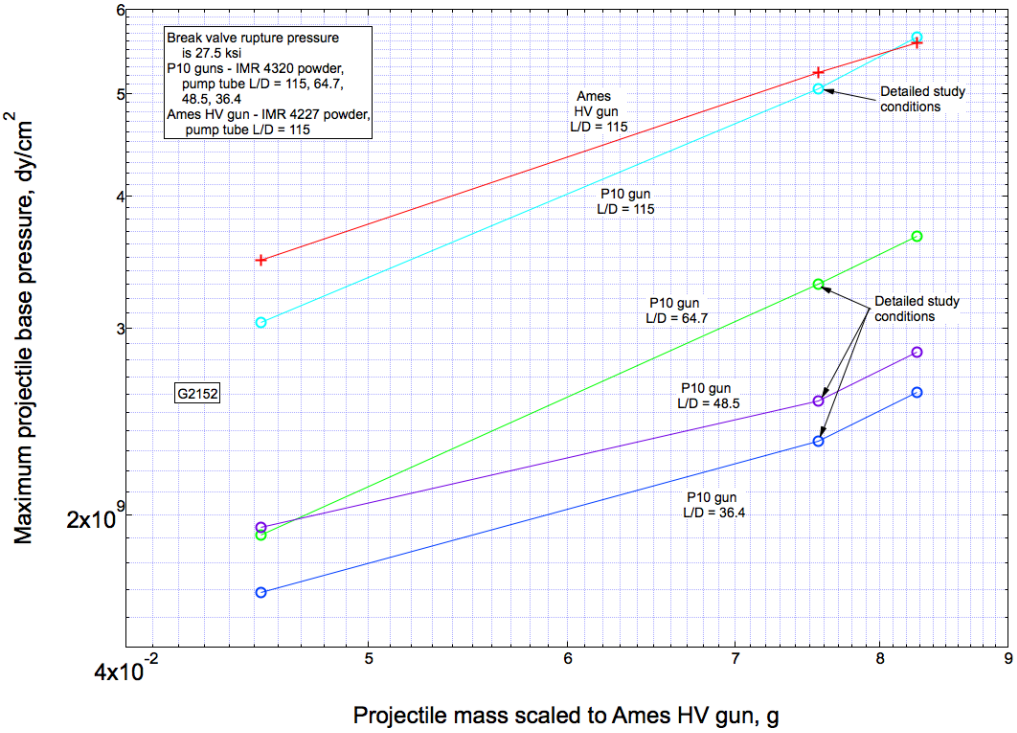

Fig. 16. Maximum projectile base pressures versus projectile mass for the P10 gun configurations with pump tube L/Ds of 115, 64.7, 48.5 and 36.4 and for the Ames HV gun for a break valve rupture pressure of 27.5 ksi.

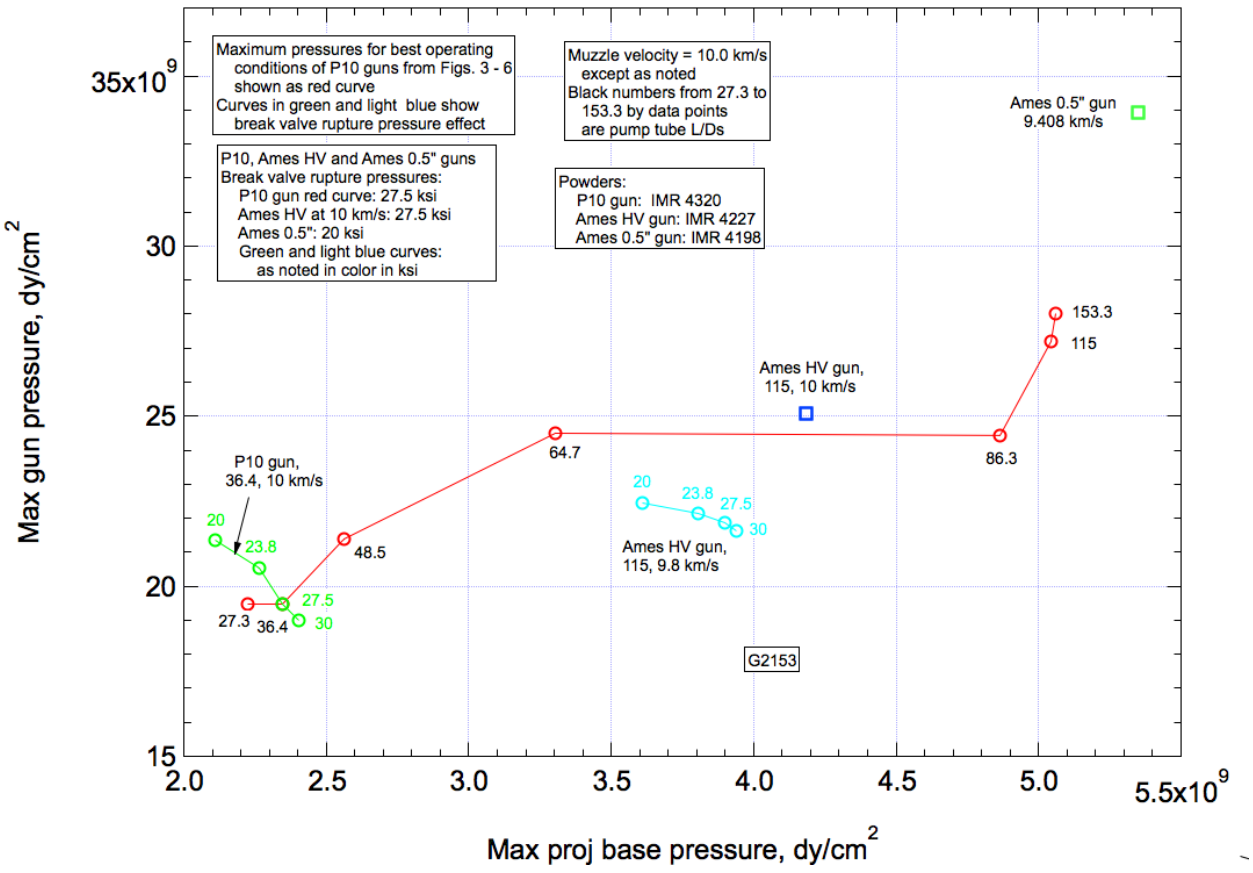

Fig. 17. Maximum model base pressures and maximum gun pressures for the optimum operating conditions for the P10 guns at 10 km/s for all pump tube L/Ds. Also shown are the CFD points for the Ames HV gun at a muzzle velocity of 10 km/sec and the Ames 0.5" gun at a muzzle velocity of 9.408 km/sec. Additional points (green and light blue) show the effect of varying the break valve rupture pressure for the P10 gun with a L/D of 36.4 and the Ames HV gun at a muzzle velocity of 9.8 km/s.

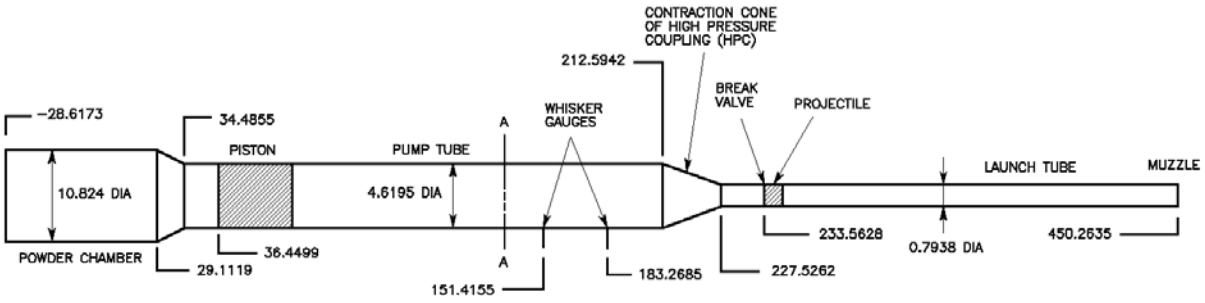

Fig. 18. P10 gun configuration for pump tube L/D of 36.4 showing dimensions (in cm). Not to scale.

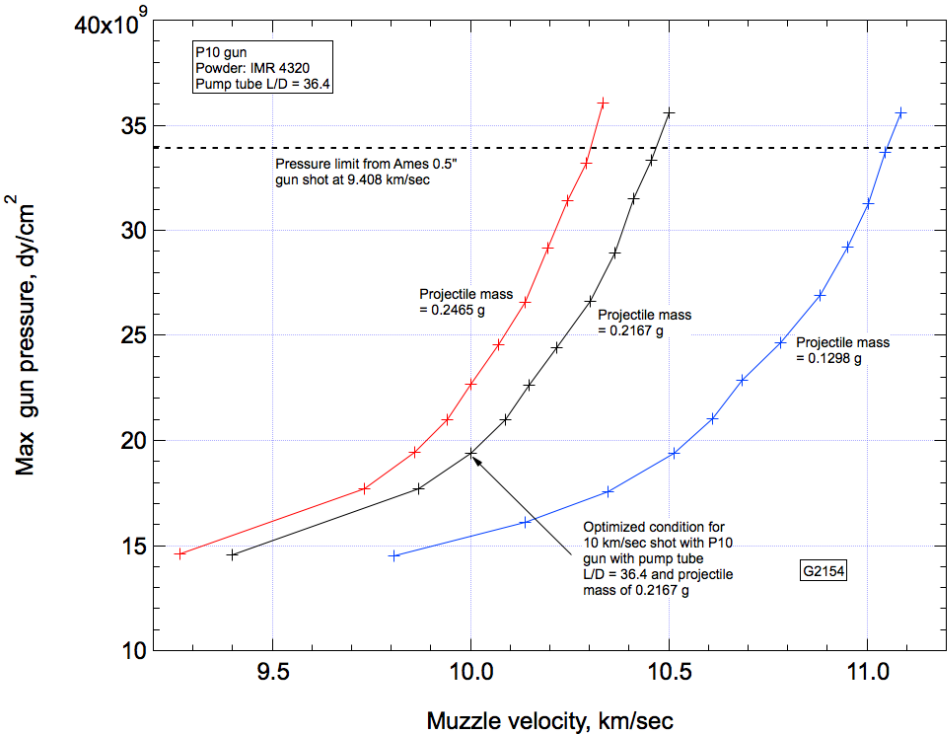

Figure 19. Maximum gun pressure versus muzzle velocity. Variations of projectile mass and powder load from starting point of optimized P10 gun for pump tube L/D of 36.4 and 10 km/sec muzzle velocity.

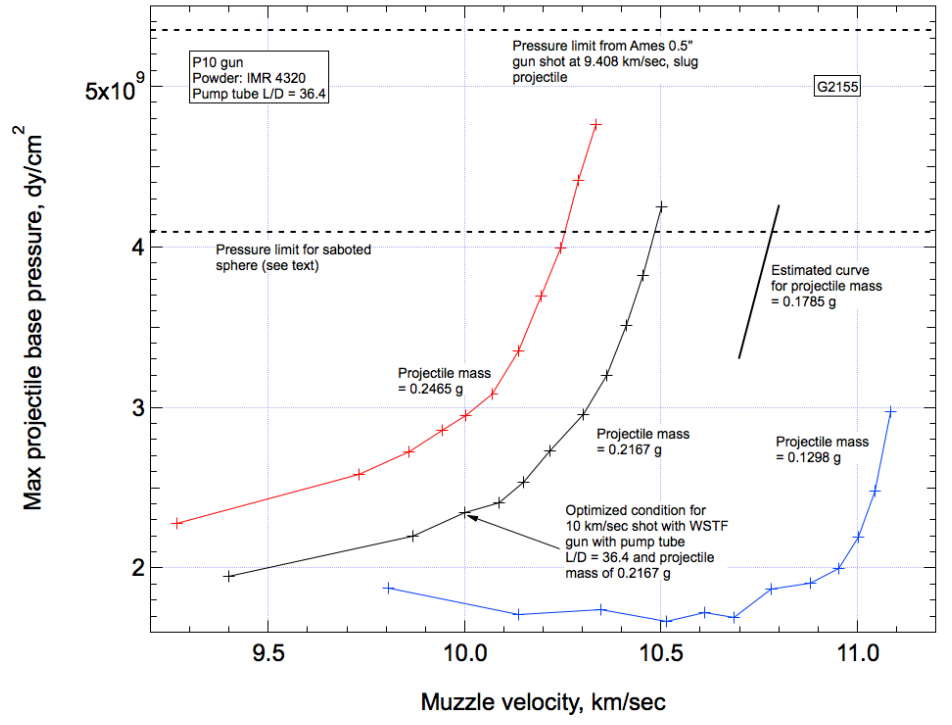

Figure 20. Maximum model base pressure versus muzzle velocity. Variations of projectile mass and powder load from starting point of optimized P10 gun for pump tube L/D of 36.4 and 10 km/sec muzzle velocity.

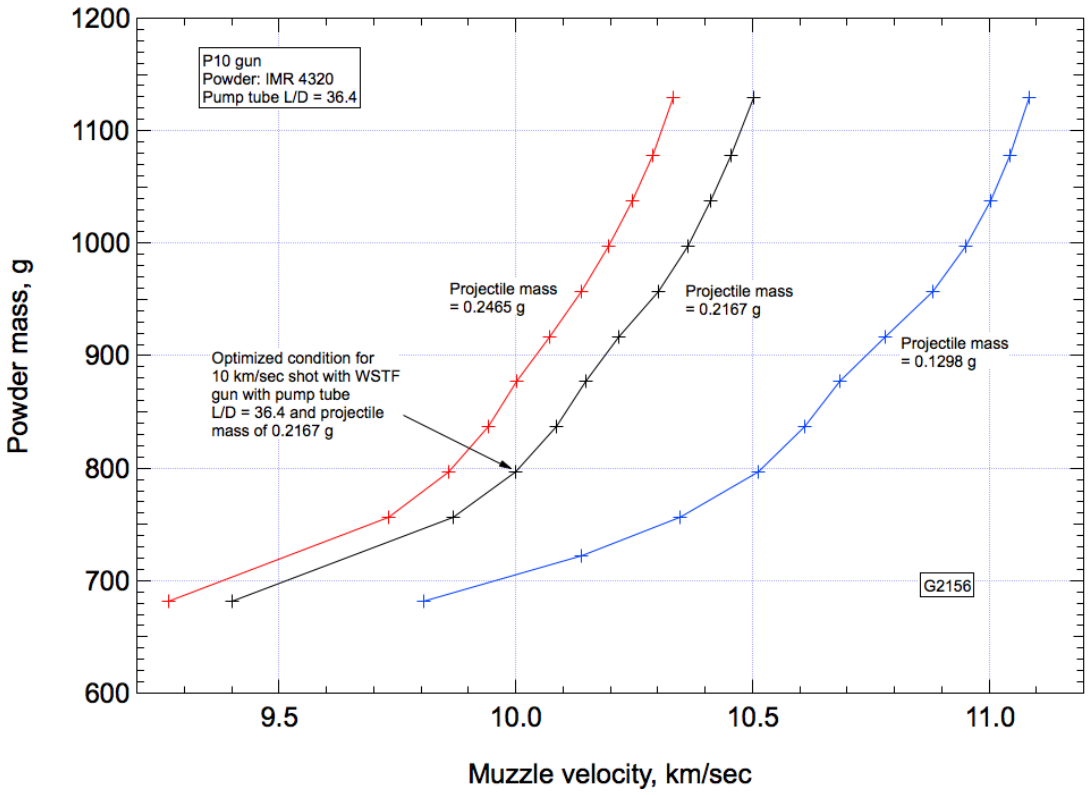

Figure 21. Powder load versus muzzle velocity. Variations of projectile mass and powder load from starting point of optimized P10 gun for pump tube L/D of 36.4 and 10 km/sec muzzle velocity.

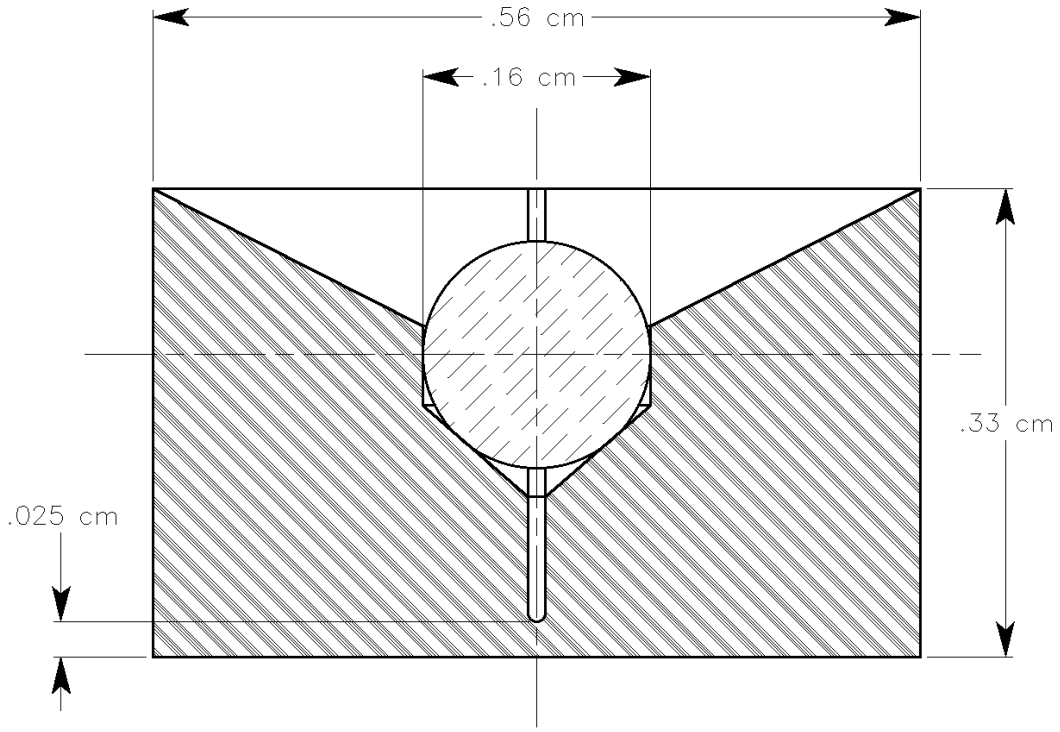

Figure 22. Sphere in sabot. Aluminum projectile, mass = 0.0060 g. Nylon sabot, mass = 0.080 g. Two cuts in sabot 90 degrees apart. Muzzle velocity = 9.4 km/sec.

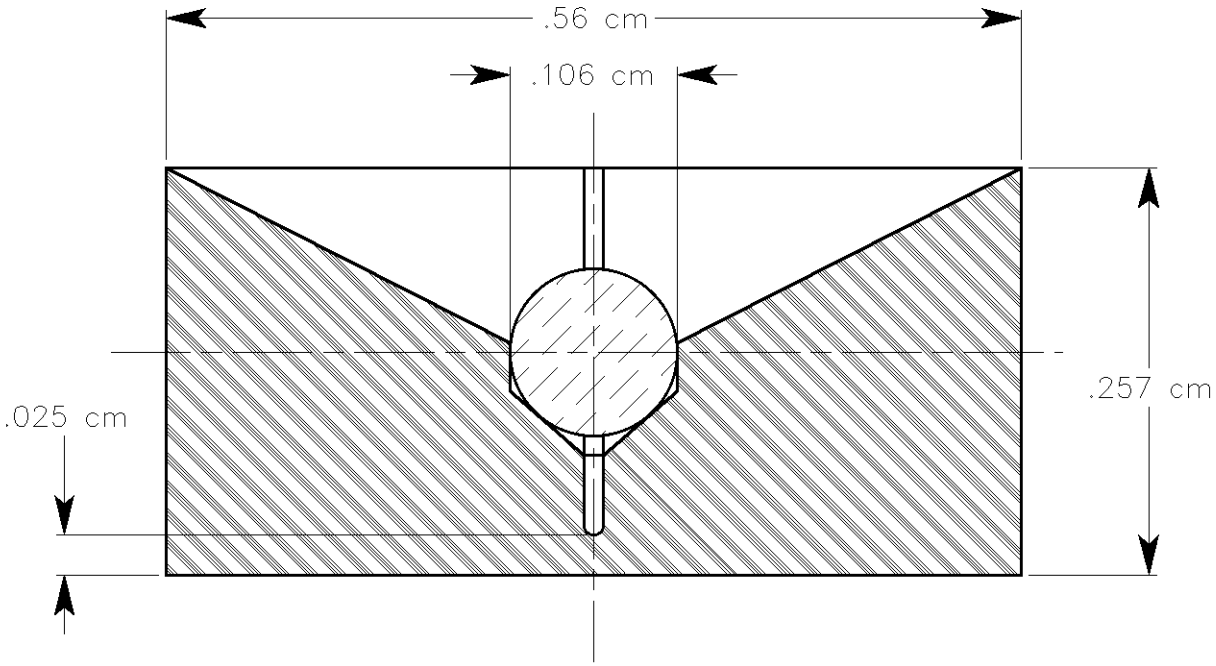

Figure 23. Concept for sabot for sphere smaller in diameter relative to the launch tube diameter than that shown in Fig. 22.